AFGL-TR-86-0139   SSS-R-86-8064

Charging of a Man in the Wake of the Shuttle

G. A. Jongeward
I. Katz
M. J. Mandell
J. R. Lilley, Jr.

S-CUBED
P.O. Box 1620
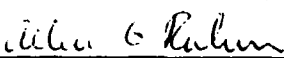La Jolla, CA 92038

AD-A182 789

July 1986

Scientific Report No. 5

AIR FORCE GEOPHYSICS LABORATORY
AIR FORCE SYSTEMS COMMAND
UNITED STATES AIR FORCE
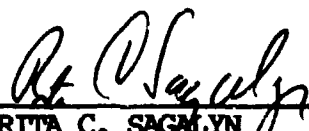HANSCOM AIR FORCE BASE, MA 01731

"This technical report has been reviewed and is approved for publication"

_____
ALLEN G. RUBIN
Contract Manager

_____
CHARLES P. PIKE, Jr.
Spacecraft Interactions Branch Chief

FOR THE COMMANDER

_____
RITA C. SAGALYN
Space Physics Division Director

This report has been reviewed by the ESD Public Affairs Office (PA) and is releasable to the National Technical Information Service (NTIS).

Qualified requestors may obtain additional copies from the Defense Technical Information Center. All others should apply to the National Technical Information Service.

If your address has changed, or if you wish to be removed from the mailing list, or if the addressee is no longer employed by your organization, please notify AFGL/DAA, Hanscom AFB, MA 01731. This will assist us in maintaining a current mailing list.

Do not return copies of this report unless contractual obligations or notices on a specific document requires that it be returned.

AD-A182789

REPORT DOCUMENTATION PAGE

1a. REPORT SECURITY CLASSIFICATION UNCLASSIFIED		1b. RESTRICTIVE MARKINGS
2a. SECURITY CLASSIFICATION AUTHORITY		3 DISTRIBUTION/AVAILABILITY OF REPORT Approved for public release; distribution unlimited.
2b. DECLASSIFICATION/DOWNGRADING SCHEDULE		
4. PERFORMING ORGANIZATION REPORT NUMBER(S) SSS-R-86-8064		5. MONITORING ORGANIZATION REPORT NUMBER(S) AFGL-TR-86-0139
6a. NAME OF PERFORMING ORGANIZATION S-Cubed	6b. OFFICE SYMBOL (If applicable)	7a. NAME OF MONITORING ORGANIZATION DCASMA, San Diego
6c. ADDRESS (City, State, and ZIP Code) P.O. Box 1620 La Jolla, CA 92038		7b. ADDRESS (City, State, and ZIP Code) 4297 Pacific Highway San Diego, CA 92110
8a. NAME OF FUNDING/SPONSORING ORGANIZATION Air Force Geophysics Laboratory (AFGL/PHK)	8b OFFICE SYMBOL (If applicable)	9. PROCUREMENT INSTRUMENT IDENTIFICATION NUMBER Contract F19628-82-C-0081

8c. ADDRESS (City, State, and ZIP Code) Hanscom Air Force Base, MA 01731	10. SOURCE OF FUNDING NUMBERS			
	PROGRAM ELEMENT NO.	PROJECT NO	TASK NO	WORK UNIT ACCESSION NO.
	62101F	7661	11	AA

11. TITLE (Include Security Classification)

Charging of a Man in the Wake of the Shuttle

12. PERSONAL AUTHOR(S) G. A. Jongeward, I. Katz, M. J. Mandell, J. R. Lilley, Jr.

13a. TYPE OF REPORT Scientific Report No. 5	13b. TIME COVERED FROM ___ TO ___	14. DATE OF REPORT (Year, Month, Day) July 1986	15 PAGE COUNT 70

16. SUPPLEMENTARY NOTATION (Computer code)

17	COSATI CODES		18 SUBJECT TERMS (Continue on reverse if necessary and identify by block number)
FIELD	GROUP	SUB-GROUP	EVA. EMU, Spacecraft Charging, Auroral Ionosphere, POLAR
			Computer Code, NASCAP Computer Code, MATCHG Computer Code,
			DMSP Satellite, Auroral Charging, Astronaut Charging,

19. ABSTRACT (Continue on reverse if necessary and identify by block number) Space-charge limited, Orbit Limited.

Charging of the DMSP F6 and F7 satellites is shown to result from the combined effects of high flux of high energy auroral electrons and low ambient background ion density. POLAR calculations are presented which show that a shuttle size object will charge more than 3000 volts negative under these charging conditions. The highly charged shuttle accelerates ions to the shuttle potential producing a high energy mono-energetic plasma environment near the shuttle. During these charging events, an astronaut performing EVA will charge with its ion collection orbit limited. Material secondary properties will produce differential charging on the astronaut of the same magnitude as the shuttle charging potential. NASCAP calculations of EMU charging in the near shuttle environment show differential voltages of 2600 volts and overall charging 1000 volts more negative than the shuttle will occur.

20. DISTRIBUTION/AVAILABILITY OF ABSTRACT ☐ UNCLASSIFIED/UNLIMITED ☐ SAME AS RPT. ☐ DTIC USERS	21. ABSTRACT SECURITY CLASSIFICATION Unclassified	
22a. NAME OF RESPONSIBLE INDIVIDUAL W. Hall	22b. TELEPHONE (Include Area Code)	22c. OFFICE SYMBOL AFGL/PHE

DD FORM 1473, 84 MAR   83 APR edition may be used until exhausted. All other editions are obsolete.   SECURITY CLASSIFICATION OF THIS PAGE

Charging of a Man in the Wake of the Shuttle

I. Introduction

This report describes a portion of the work performed by S-CUBED under the contract AFGL-F19628-82-C-0081 which pertained to charging of an astronaut performing EVA. The report covers work in which the charging of the DMSP satellites is studied and shown to be understood using classical models of ion collection. The physics of coupled large (shuttle) and small (EMU) object charging in strong auroral environments which was developed by S-CUBED researchers is presented here. From this understanding, the POLAR, NASCAP, and MATCHG codes were used in conjunction to calculate the charging of the EMU in the auroral environments measured by the DMSP satellites F6 and F7. These calculations are reported here. Much of the material presented in this report has been presented elsewhere or given in the interim report presented at the Janurary 1986 Reno AIAA meeting.

The DMSP satellite has been observed to charge to potentials as large as 679 volts negative with respect to the local plasma. This occurred when the environment was a combination of an intense auroral electron precipitation combined with a dropout of the ambient cold plasma density. Previous calculations using the POLAR and NASCAP models of spacecraft charging demonstrated that the measured environments, when used as input to the codes, predicted charging to the levels observed. Calculations of charging by an isolated EMU were consistent with the DMSP results. Further calculations were performed, using POLAR, which showed that charging by shuttle sized objects is much more severe than for the smaller satellites. An environment which would charge DMSP to -172 Volts was calculated to charge the a shuttle-sized object to -3545 Volts. However, no theory or code was adequate to calculate the overall and differential potentials on the EMU during EVA in the vicinity of the shuttle. This paper discusses such a theory, and by using a combination of computer codes is able to present calculations of EMU charging during shuttle EVA.

In section II. an analysis of the charging of the DMSP satellite is presented using the MATCHG code. The MATCHG code is a zero dimensional code which has an orbit limited current collection model and the sophisticated models of surface secondary and backscatter currents contained in the NASCAP code. The MATCHG analysis of DMSP charging matches qualitatively and quantitatively the measured charging without any free parameters. A scaling from small DMSP

1

size objects where the current collection is orbit limited to larger shuttle size objects where the current collection is space charge limited is presented. Under DMSP environments the shuttle is shown to charge in excess of 3000 volts negative. In section III. the physics of shuttle EMU charging is discussed. Under the effects of the strong auroral environments seen by the DMSP satellites, the shuttle is shown to produce a high energy mono-energetic ion environment for the EMU. The energy of incoming ions is approximately the shuttle potential. Differential charging between the EMU and shuttle and between different materials on the EMU is shown to be a substantial fraction of the shuttle potential. In section IV. POLAR calculations of the shuttle charging in the DMSP environments are presented. The calculations show that the shuttle charges to -3290 volts. In section V. MATCHG calculations of EMU materials in the mono-energetic environment determined in section IV are presented. These calculations show that charging of the EMU to over 6000 volts negative will occur and differential charging of over 2000 volts is expected. In section VI. NASCAP is used to model the detailed charging of the EMU under the shuttle induced environments determined in sections IV. and V.. The NASCAP calculations confirm the MATCHG calculations in magnitude of charging and reveal that the parts of the suit will charge much slower than the rest of the materials. The final section, VII, gives estimates of the energy stored, capacitively, in the EMU due to absolute and differential charging.

II. Analysis of DMSP Charging

The following paper titled "ANALYSIS OF DMSP CHARGING AND IMPLICATIONS FOR POLAR SHUTTLE MISSIONS" was presented at the AIAA shuttle environment interactions workshop held in Houston, Tx in November 1985. The paper contains an analysis of the observed DMSP F6 and F7 satellite charging. The DMSP satellite charged to hundreds of volts negative during eclipse conditions of high auroral electron flux and low ambient ion density. The analysis presented shows that the ion current collection is orbit limited for a small object such as DMSP and will become space charge limited for shuttle size objects. The MATCHG code, which assumes orbit limited current collection and has NASCAP's models of surface secondary generation, was used to predict the DMSP charging potentials using as input the observed environments as presented by Gussenhoven et.al.[1] The MATCHG predictions of the DMSP charging potentials are shown to agree with the observed charging potentials if the ion species is assumed to be Oxygen. For a hydrogen ion environment, the predicted charging of the DMSP satellite is shown to be much lower than observed.

ANALYSIS OF DMSP CHARGING AND THE IMPLICATIONS FOR
POLAR SHUTTLE MISSIONS

I. Katz, M. J. Mandell, G. A. Jongeward, J. R. Lilley, Jr.
S-CUBED
La Jolla, CA 92038

William N. Hall, M. S. Gussenhoven
Air Force Geophysics Laboratory
Hanscom Air Force Base, MA 01731

The high levels of spacecraft charging seen on DMSP/F6 and DMSP/F7 resulted from the combination of high fluxes of auroral electrons and a low background ambient density. Calculations are presented using MATCHG, a material charging code, which show the observed satellite charging events are consistent with the measured auroral environments. Full three-dimensional calculations using the POLAR code with these environments show that a shuttle size object would charge to thousands of volts.

Introduction

High levels of spacecraft charging have been observed on at least two satellites, DMSP/F6 and DMSP/F7, in 840 km polar orbit.[1,2] When charging occurred, the satellites' environments were characterized by intense fluxes of high energy auroral fluxes and by particularly low densities in the low energy ambient plasma. Calculations using MATCHG[3], a spacecraft charging model, show that the observed levels of charging are consistent with the measured environments. The model includes secondary and backscattered electrons, which make up more than half of the positive currents to the satellite. The assumption that the ambient plasma consists primarily of oxygen ions is fundamental to the agreement with experiment. Collection of ions by DMSP is shown to be orbit limited.

5

For larger objects, such as the shuttle or an astronaut near the shuttle, space charge effects will cause substantially greater charging. Three-dimensional calculations using the POLAR code show charging of the shuttle in excess of a 3000 volts negative will occur from the auroral events seen by DMSP. Even at higher ion densities more common to shuttle altitudes, charging in excess of 1000 volts negative will occur.

DMSP Charging Calculations

The DMSP charging calculations were performed using the MATCHG code for the three environments for which fits to the high energy auroral electron fluxes were provided in Reference 1. As a worst case scenario, the observation with the most intense auroral flux was chosen as a fourth case to calculate. The auroral flux above 14 keV was 9.4 x 10^9 $(cm^2 s-sr)^{-1}$ for DMSP/F6 on January 12, 1983. In the absence of a spectral fit, the high energy electrons were assumed to have a temperature of 10.1 keV, the same as the highest intensity case with a fit reported. For this case, the high energy auroral electron density used was

$$n = \frac{J_{observed}}{e\sqrt{\frac{\theta T}{2\pi m}}} \qquad (1)$$

with $J_{observed}/e = 9.4 \cdot 10^9/cm^2/s-sr$. This gives the value for n of $32/cm^3$ displayed in Table 2.

The MATCHG code assumes orbit limited current collection. This approximation is valid when the dominant current limiting mechanism is

the conservation of angular momentum of the collected particles. For a
DMSP size object, the observed charging potentials and ambient
environment produced orbit limited conditions. A discussion of the
crossover size from orbit limited to space charge limited collection
will be deferred to the next section. In this section we will assume
current collection is orbit limited. The orbit limiting mechanism is
depicted in Figure 1 for isotropic and flowing plasmas. For the flowing
plasma experienced by DMSP, a ram ion with energy ϕ_{ram} will be collected
by the satellite providing angular momentum conservation,

$$r_{sheath} \, v_{ram} = r_{sat} \, v_{sat}$$

and energy conservation,

$$q\phi_{ram} = m_{ion} \frac{v_{sat}^2}{2} + q\phi_{sat}$$

can be satisfied where

$$\phi_{ram} = \frac{1}{2} \frac{m_{ion}}{q} v_{ram}^2 \quad .$$

Solving these simultaneous equations gives the radius for ion
collection, r, the current to the satellite is then,

$$I(\phi) = 2\pi r^2 J_{ram}$$

where J_{ram} is the ram ion current density. Finally,

$$I(\phi) = 2\pi r_{sat}^2 J_{ram} \left(1 + \frac{\phi}{\phi_{ram}} \right)$$

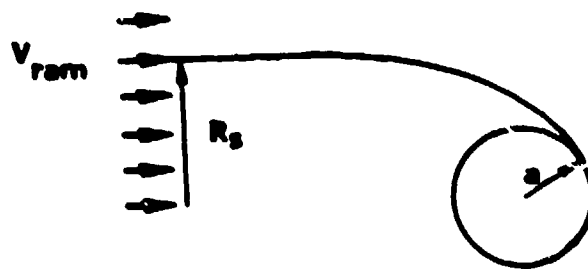This is the form for the surface current used by the MATCHG code.

Figure 1.   Orbit limited collection from   a flowing plasma with velocity V_{ram}.

MATCHG models the   satellite as a   sphere   covered with a single material.   The calculations were done assuming teflon, since teflon beta cloth is a typical external   covering of   low altitude spacecraft.   The external surface material   determines   the   secondary and backscattered electron currents which cancel   over   three-fourths   of   the incident auroral electron flux.   Table 1 shows   the different components of the current before charging and near equilibrium.

The top half of Table 1 gives the initial charging components corresponding to the uncharged DMSP satellite at 0. volts. The lower half shows the charging components for the equilibrium potential reached by the satellite. Note that this final potential represents a four order of magnitude reduction in the charging currents. The charging, in this case to -295 volts, perturbs the electron flux only slightly. The ion current has increased sixty fold to achieve current balance.

Table 1. MATCHG Calculation of the Charging of a Teflon Sphere

Potential 0. E+00 Volts

Incident Electron Current	-1.05E-05
Secondary Electrons	4.92E-06
Backscattered Electrons	2.98E-06
Incident Proton Current	3.83E-08
Secondary Electrons	3.96E-10
Bulk Conductivity Current	0.00E+00

Net Current -2.59E-06 amps/m^2

Potential -2.95•E02 Volts

Incident Electron Current	-1.02E-05
Secondary Electrons	4.78E-06
Backscattered Electrons	2.90E-06
Incident Proton Current	2.40E-06
Secondary Electrons	1.49E-07
Bulk Conductivity Current	2.32E-10

Net Current -6.36E-10 amps/m^2

The final voltage of -302 corresponds to a four order of magnitude reduction in charging current.

The charging results for all four cases are shown in Table 3. The environments used for comparison with experiment are shown in Table 2. In all cases the ram energy was taken to be 4.76 eV corresponding to oxygen at orbital velocities.

9

Table 2. Environments Used for MATCHG Calculations

n_i	n_e	T_e (keV)
125	3.9	10.1
190	3.2	14.4
180	4.9	4.2
537	32.0	10.1

As has been seen in studies of spacecraft charging at geosynchronous orbit, charging requires high electron temperatures as well as intense currents. The third case did not charge because a 4.2 keV Maxwellian spectrum generates more secondary and backscattered electrons on a teflon surface than incident electrons.

Table 3. MATCHG Charging Calculations for Spacecraft Potential ϕ_{SC} Compared with Observation. The fit to the F6 data is discussed.

Satellite	UT	ϕ_{SC} (Observed)	ϕ_{SC} (Predicted)
F7 11/26/83	49843	-317	-295
F7	49844	-140	-284
F7	49845	- 44	-0
F6' 1/12/83	35877	-462	-532

*Data fit by authors (see text)

Further studies were performed to evaluate the sensitivity of the charging to the choice of spacecraft external material and to the assumption of an oxygen plasma. Table 4 shows the charging levels for four different spacecraft materials. Except for gold, which did not charge, the three other materials responded similarly. Because gold has a high atomic number it is relatively easy to produce secondary electrons which escape preventing charging. Kapton, which has been observed on SCATHA[4] to charge strongly, shows charging even for the mildest environment. The level of charging of all three dielectric coatings were comparable with experiment.

Table 4. Calculations Using MATCHG for Gold, Kapton, Teflon, and Indium Oxide Spheres Showing the Predicted Charging Levels for the Three Spectral Fits from Reference 1.

Ram Oxygen Plasma

Electrons		Oxygen					
N [cm^{-3}]	T [keV]	N [cm^{-3}]	T [eV]	Gold	Kapt	Tefl	Indo
3.9	10.1	125	4.76	+0.4	-551	-295	-370
3.2	14.4	140	4.76	-8.9	-434	-284	-301
4.9	4.2	180	4.76	+1.4	-163	+0.5	-11.7

The predicted levels of charging change dramatically if the environment is assumed to be dominated by hydrogen ions. As seen in Eq. (3), for satellite potentials more than a few volts negative the collected ion current is inversely proportional to the mass of the ion. To collect the same ion current in a hydrogen plasma requires only 1/16 the potential as an oxygen plasma. As seen in Table 5, the equilibrium voltages for a spacecraft in a hydrogen plasma are an order of magnitude down from those for an oxygen plasma. Even if the ion temperature is assumed to be 1 eV, the predicted potentials for all materials are far below those observed on DMSP.

Table 5. Calculations Using MATCHG Showing the Low Level Charging Predicted for a Hydrogen Background Plasma of Hydrogen.

Thermal Hydrogen Plasma

Electrons		Hydrogen					
N [cm^{-3}]	T [keV]	N [cm^{-3}]	T [eV]	Gold	Kapt	Tefl	Indo
3.9	10.1	125	0.3	+0.4	-35.8	-17.8	-22.7
3.9	10.1	125	1.0	+0.4	-64.2	-31.9	-40.6
3.2	14.4	190	0.3	-0.5	-26.1	-16.8	-17.9
3.2	14.4	190	1.0	-0.4	-46.9	-30.0	-32.0
4.9	4.2	180	0.3	+1.4	- 9.7	+ 0.5	- 0.6
4.9	4.2	180	1.0	+1.4	-17.2	+ 0.5	- 0.7

MATCHG assumes orbit limited collection of both electron and ions. Orbit limited collection of the energetic electrons is easily justified. For the ions, orbit limited theory will also be valid if the orbit limited collection radius is less than the space charge limited sheath distance for collection of the same ion current density at the final voltage.

The orbit limited and space charge limited sheath distances for three spherical objects with radii 0.5 m, 1 m, and 15 m are given in Table 6. The first two radii are approximately DMSP size objects while the 15 m radius represents a shuttle size object. The orbit limited sheath radius is determined by angular momentum conservation

$$r_{sheath} = r_{satellite} \sqrt{1 + \frac{|\phi_{sat}|}{\phi_{ram}}}$$

where ϕ_{ram} is the ram ion kinetic energy. $\phi_{ram} = mV^2/2q$. For oxygen in an 800 km orbit, ϕ_{ram} is 4.76 volts. Detailed three-dimensional calculations using the POLAR[5] code indicate that the ram flux produces an approximate isotropic flux with magnitude $\pi r_{sat}^2 \, J_{ram} = 4\pi r_{sat}^2 \, J_i$. Using this value for the flux over an entire spherical sheath boundary gives the space charge limited radii listed in Table 6.[6]

Table 6. Comparison of the Orbit Limited and Space Charge Limited Sheaths for Two Satellite Size Objects and One Shuttle Size Object

Satellite	UT	ϕ_{SC} [V] (Observed)	n_{ion} [cm^{-3}]	Spacecraft Radius [m]	Orbit Limited Sheath Radius [m]	Space Charge Limited Sheath Radius [m]
F7	49843	-317	125	0.5	4.2	8
				1.0	8.4	11
				15.0	125.0	42
F7	49844	-140	190	0.5	2.8	5.5
				1.0	5.6	7
				15.0	85.0	30
F7	49845	-44	180	0.5	1.6	3.3
				1.0	3.2	4.6
				15.0	48.0	23
F6	35877	-462	537	0.5	5.1	6.5
				1.0	10.1	8.6
				15.0	152.0	35

Because the orbit limited sheath is within the range of space charge limited sheath sizes, an orbit limited calculation such as MATCHG is appropriate for small objects such as DMSP. However, for larger objects, such as the space shuttle, it is seen that the current collection is strongly space charge limited.

Space Charge Limited Collection

As is seen in Table 6 and Eq. (3), the radius for orbit limited current collection is proportional to the spacecraft radius. Hence, under orbit limited conditions a spacecraft's equilibrium potential is independent of its size, because the surface ion flux is independent of the spacecraft radius

$$j_{surface} = r^2_{sheath}/r^2_{sat} \cdot \left[1 + \frac{|\phi_{SC}|}{\phi_{ram}} \right]$$

This result is valid for small objects. For larger objects, the collected current produces enough space charge to shield the spacecraft's potential, limiting its collection ability. This spacecharge shielding distance introduces a new length scale into the physics. So the size invariance of the equilibrium potential which existed for orbit limited collection is no longer true.

For spherical objects a different size scaling can be determined by examining Poisson's equation including the space charge contribution. For completeness this scaling argument is reviewed in Appendix A. The result, Eq. (A.3) in the appendix, is 2. Spacecraft with sizes L_1, L_2 will have equilibrium potentials related by $V_1/V_2 = (L_1/L_2)^{4/3}$. This effect is reflected in Table 6 where the space charge limited sheath distance scales much slower than the spacecraft radius. For example, in the auroral environments seen by DMSP, a two meter radius object (a 2 meter size object is just beginning to be affected by space charge shielding) charged to a few hundred volts. In contrast, a shuttle size object (approximately 15 meters in radius) would charge according to Eq. (A.3) to

$$V_{shuttle} = (15/2)^{4/3} V_{2m} = 15 \ V_{2m} \tag{4}$$

A shuttle size object will charge than an order of magnitude more than a 2 meter size object in the same environment.

Shuttle Collection and Astronaut Charging

The calculations of auroral charging on shuttle size objects were accomplished using the POLAR computer code. The POLAR code is a three-dimensional code which computes the potentials on and about a large object (with respect to the Debye length) accounting for space charge, spacecraft wakes, secondary electrons and backscatter. The auroral environments used are given in Table 7. The first environment corresponds to the observation on DMSP/F7 at 49843 UT. The second environment is the "strongest" auroral environment which was used previously with the MATCHG calculations, except the density of the cold ions has been increased to $10^4/cm^3$, a more typical value for a 300 km polar orbiting shuttle.

Table 7. Charging of a Shuttle-size Object

$n_e(cm^{-3})$	$kT_e(1eV)$	$n_i(cm^{-3})$	$\phi_{SC}(V)$	(ϕ_{small})
3.9	10.1	125	-3290	(-172)
32	10.1	10^4	-1306	(-23)

The model used in the POLAR calculations had the approximate size and shape of the actual shuttle and is shown in Figure 2. Teflon was chosen as a covering material for the model because it has similar secondary characteristics as the shuttle insulating tiles. The computational space was a cubical mesh of size 3.5 meters and an overall grid size of (120 meters).[3] Although this model is a crude rendition of the actual shuttle, the bulk charging results are reliable because the size attributes and material properties are comparable.

The results of the POLAR calculations along with the environments are given in Table 7. The column ϕ_{SC} is the POLAR result for the equilibrium potential of the shuttle size object. The final column, given for comparison, is the potential to which a DMSP size object would have charged in the same environment. The charging of shuttle size objects is seen to be, as expected, much more severe than for smaller objects.

Figure 3 shows the potential contours from the POLAR calculation. The view is from the side with the shuttle nose at the top of the figure. The motion of the shuttle is to the left. Because of the high charging potential, the sheath is spherical and far from the shuttle. The flowing ions from the ram direction were able to reach the wake side of the shuttle. This produced a spherical distribution of ions masking much of the ram wake effects. For this auroral environment the shuttle charged more than 3000 volts negative.

The potential contours for the second POLAR calculation are presented in Figure 4. For this higher cold ion density the shuttle charging was less severe but still greater than 1500 volts negative. The sheath is much closer to the shuttle and larger ram wake differential charging is predicted, although the difference was less than 250 V since this simple model assumed the shuttle was covered with a single material. Experience from spacecraft charging at geosynchronous orbit shows differential potentials arise primarily from the responses of different materials.

It is important to realize that an astronaut performing EVA during this auroral event would charge to similarly high potentials depending on his location with respect to the shuttle. Far from the shuttle, being a small object, an astronaut would charge to potentials similar to DMSP. Near the shuttle, however, charging to high levels comparable to

16

the shuttle would occur. For the low background density case, an astronaut would experience little ram wake differences. Ram wake differences increase with increasing background density.
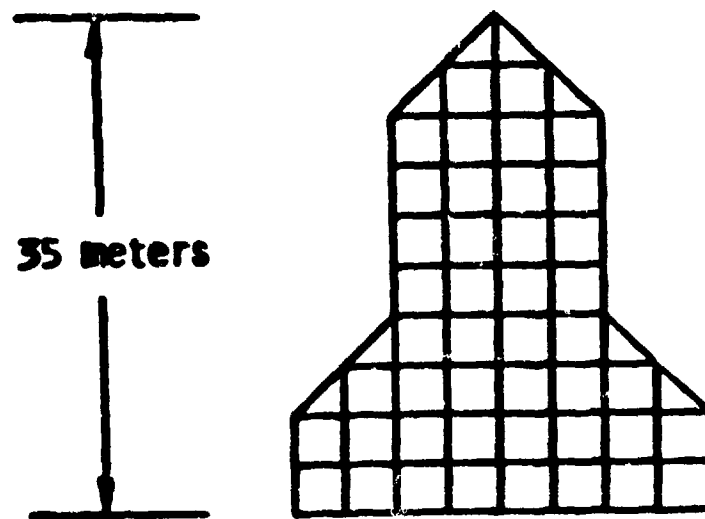
Figure 2.   Shuttle mode used in the POLAR calculations.

Contour-Level Volts

-3536.138

-3500.000

-3000.000

-2500.000

-2000.000

-1500.000

-1000.000

-500.000

-100.000

-50.000

-10.000

-1.000

1.000

OBJECT GRID UNITS
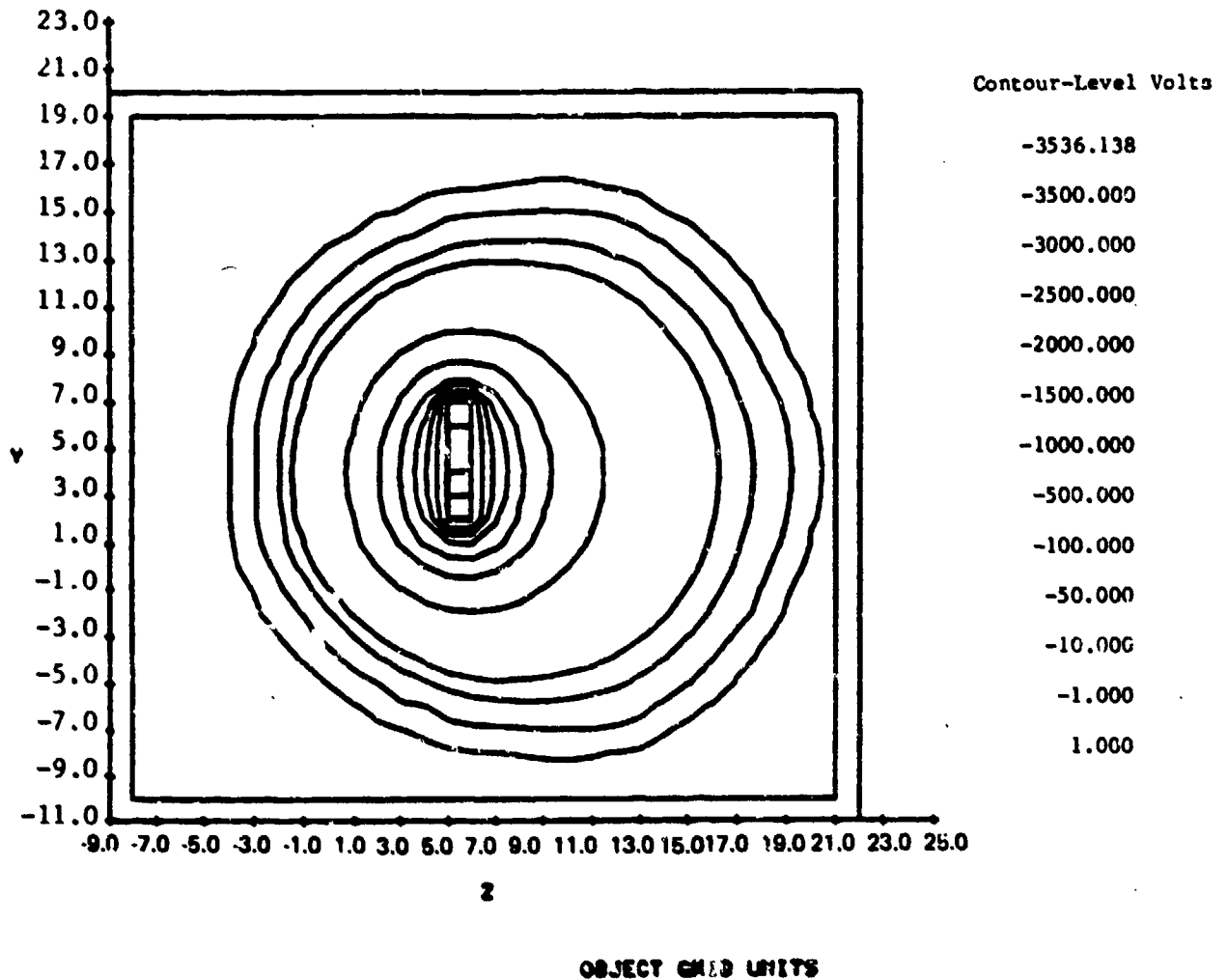
Figure 3. Potential contours for shuttle charging in an auroral environment with $n_e = 3.9$ cm^3, $kT_\circ = 10.1$ keV, $n_i = 125/$cm^3.

19
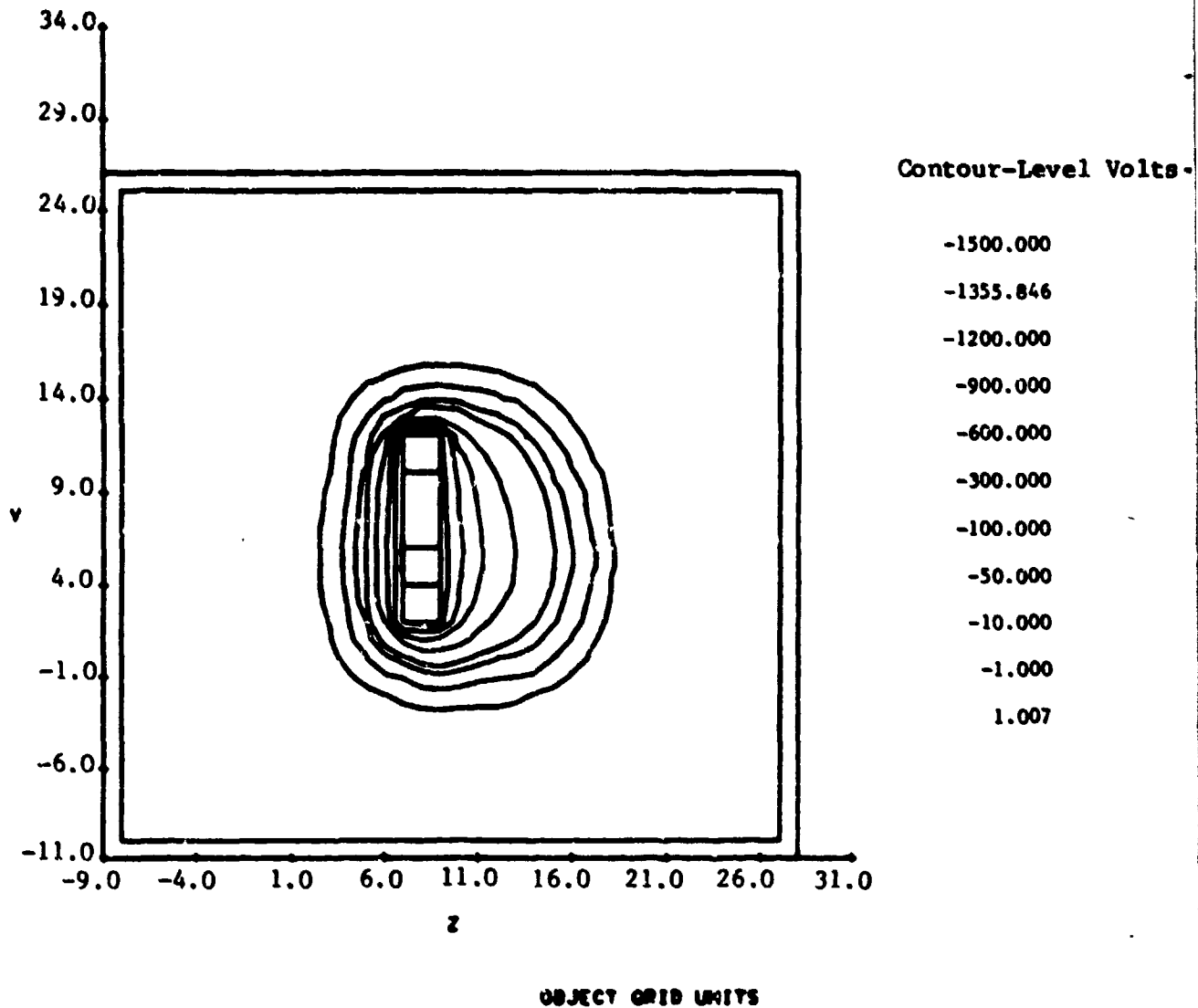
Figure 4. Potential contours for shuttle charging in an auroral environment with $n_e = 32/cm^3$, $k\bar{T}_e = 10.1$ keV, $n_i = 10^4/cm^3$.

Conclusion

The POLAR calculations presented showed that shuttle size objects will charge to thousands of volts in the DMSP observed environments.

Acknowledgment

References

1. Gussenhoven, M. S., D. A. Hardy, F. Rich, W. J. Burke and H.-C. Yeh, "High-Level Spacecraft Charging in the Low Altitude Polar Auroral Environment," AFGL-TR-85-0291, ADA162145.

2. Yeh, H.-C., M. S. Gussenhoven, D. A. Hardy and F. J. Rich, "Spacecraft Charging in the Polar Ionosphere: DMSP Eclipse Charging and Implications," ADA114426.

3. Stannard, P. R., G. W. Schnuelle, I. Katz and M. J. Mandell, "Representation and Material Charging Response of GEO Plasma Environments," Spacecraft Charging Technology-1980, NASA-CP-2182, AFGL-TR-81-0270, pp. 560-568, 1981, ADA114426.

4. Mizera, P. F. and G. M. Boyd, "Satellite Surface Potential Survey," Spacecraft Charging Technology-1980, NASA CP-2181, AFGL-TR-81-0270, pp. 461-469, 1981, ADA114426.

5. Cooke, D. L., I. Katz, M. J. Mandell, J. R. Lilley, Jr. and A. J. Rubin, "A Three-Dimensional Calculation of Shuttle Charging in Polar Orbit," Spacecraft Environmental Interactions Technology-1983, NASA-CP-2359, AFGL-TR-85-0018, pp. 205-227, 1985.

6. Parker, L. W., "Plasmasheath-Photosheath Theory for Large High-Voltage Space Structures," in Space Systems and Their Interactions with Earth's Space Environment, Progress in Astronautics and Aeronautics, Editors: H. B. Garrett and C. P. Pike, Vol. 71, p. 477, 1980.

Appendix
Potential Scaling for Space Charge Limited
Collection

Taking a plasma with temperature T, and density N, for Poisson's equation

$$\nabla^2 \phi = -\rho(\phi)/e_o = -ne \sqrt{\frac{T}{4\pi\phi}} \left[\frac{r_{sheath}}{r}\right]^2 \qquad (A.1)$$

Equation (A.1) is valid for potentials much larger than the plasma temperature because the repelled species has been ignored. Let $\phi(R_{sat}, 1)$ denote a solution to Eq. (A.1) with boundary conditions appropriate to a satellite of radius R.

$$\phi(R_{sat}, 1) = \phi_{sat}$$

$$\phi(R_{sheath}, 1) \to 0$$

It is straightforward to check by substitution into Eq. (A.1) that

$$\phi(r,b) = b^{4/3}\phi(r/b, 1)$$

is a solution to Poisson's equation corresponding to a satellite b times as large, with a sheath b times farther away, that is,

$$\nabla^2 \phi(r,b) = -ne \sqrt{\frac{T}{4\pi\phi(r,b)}} \left[\frac{br_{sheath}}{r}\right]^2$$

$$\phi(bR_{sat}, b) = b^{4/3}\phi(R_{sat}, 1) \qquad (A.2)$$

$$\phi(bR_{sheath}, b) = b^{4/3}\phi(R_{sheath}, 1) \to 0$$

23

Hence as the object size increases the object potential $\phi(bR_{sat},b)$, must increase to keep the surface flux constant. By Eq. (A.2), given two spacecraft with sizes L_1 and L_2 their equilibrium potentials will be related by

$$\frac{V_1}{V_2} = \left[\frac{L_1}{L_2}\right]^{4/3} \qquad\qquad \text{(A.3)}$$

III. The Physics of Shuttle EMU Charging

Background

Figures 1 and 2 show the POLAR models of the shuttle and EMU used during the calculations. The combined, multiple grid model is shown in Figures 3. It is immediately apparent that the EMU is extremely small compared with the shuttle. Indeed examination of the space potentials for the combined system, Figure 4, shows that the electric fields due to the EMU are not felt a few EMU radii from the EMU. The theory presented below shows that ion trajectories are modified only slightly by the presence of the EMU. It is also shown that for the EMU to collect the ion current density needed to balance auroral fluxes, the EMU charges to much higher potentials when near the shuttle than when isolated. The quantatative theory predicts differential charging potentials comparable with overall charging values.

Surface Charging Physics

The primary cause for differential charging on an object as small as the EMU is the differing secondary and backscatter currents of the various surface materials. The charging current to each surface is the difference between the incident electron current and the outgoing secondary and backscattered currents. For a given distribution of electron energies there can be a large range of net charging currents depending upon the surface material. For the intense energetic auroral electron fluxes, some materials such as gold emit about one electron for each incident electron; others, such as kapton, emit only a third the incident electrons. The surfaces charge negatively until the difference between incident and emitted electrons is made up by ions. Thus for objects with varying surface materials the ion current density must also vary along the surface. This requires the surface potentials to vary accordingly. The question of how the surface current density varies as a function of voltage distribution has been addressed previously for current collection by high voltage solar arrays. That work is extended here to calculate ion collection by a very small object in the presence of a large ion collecting object.
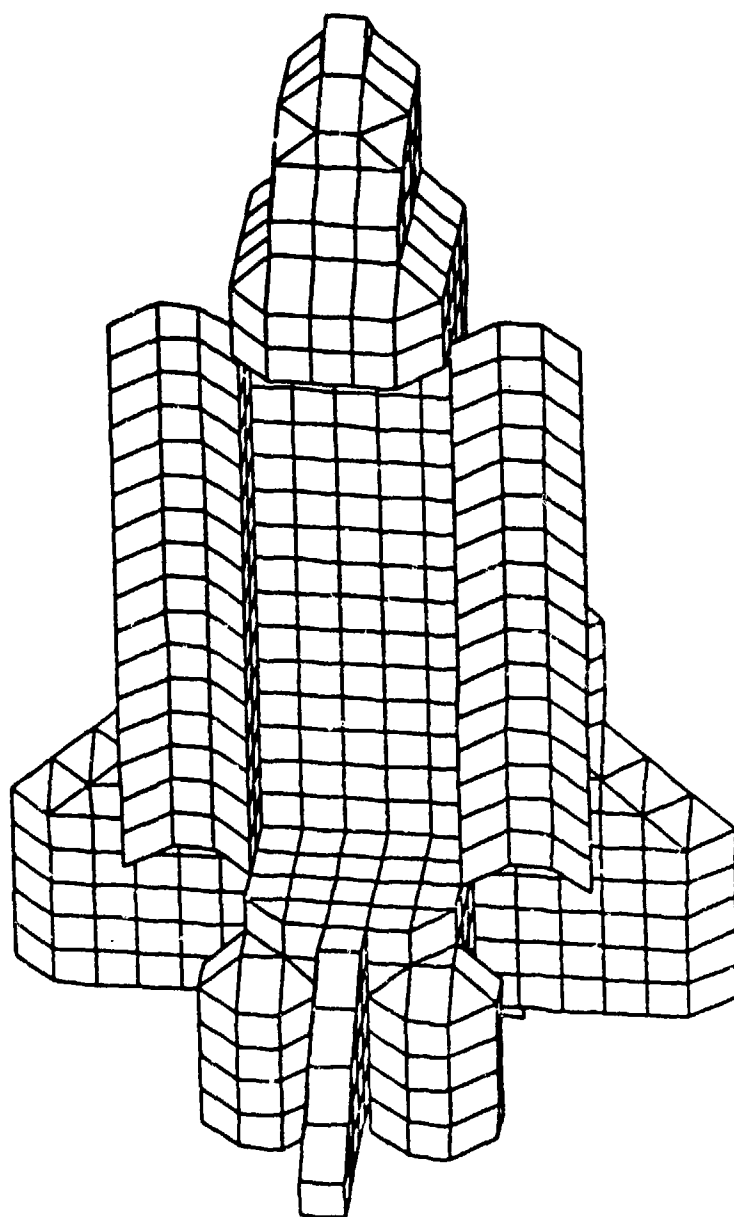
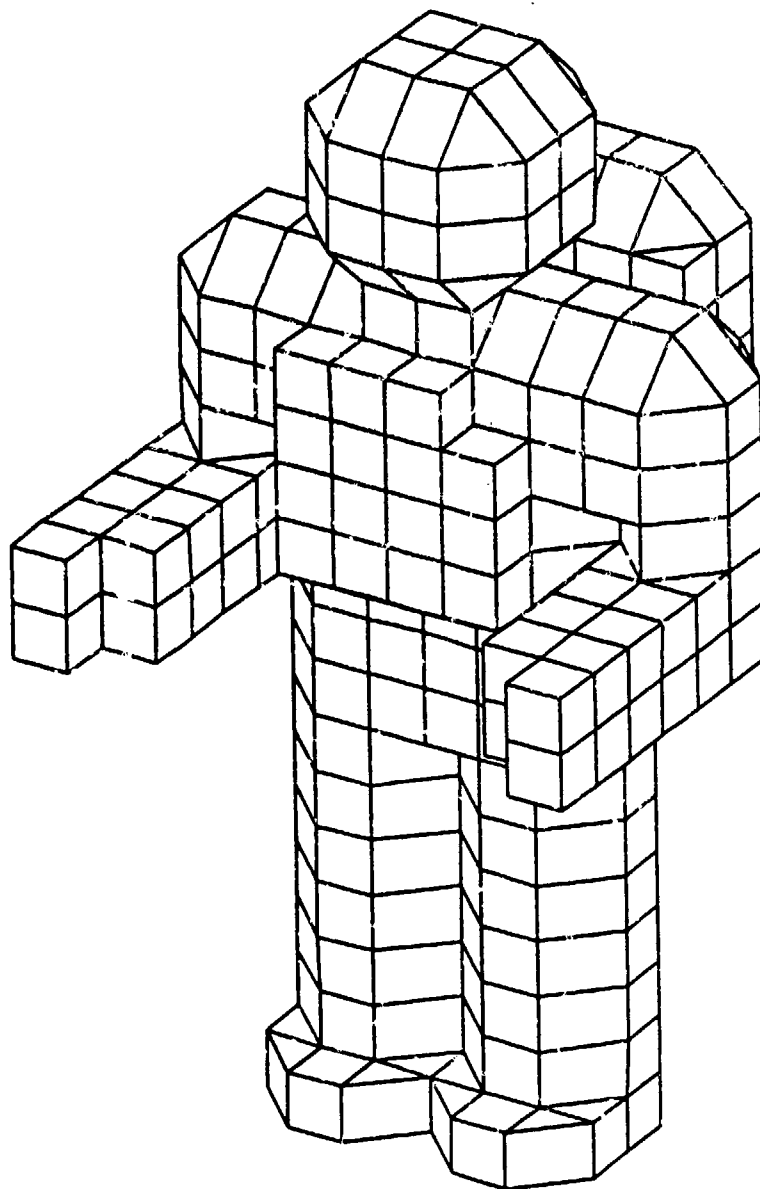Figure 1. POLAR Model of Shuttle.
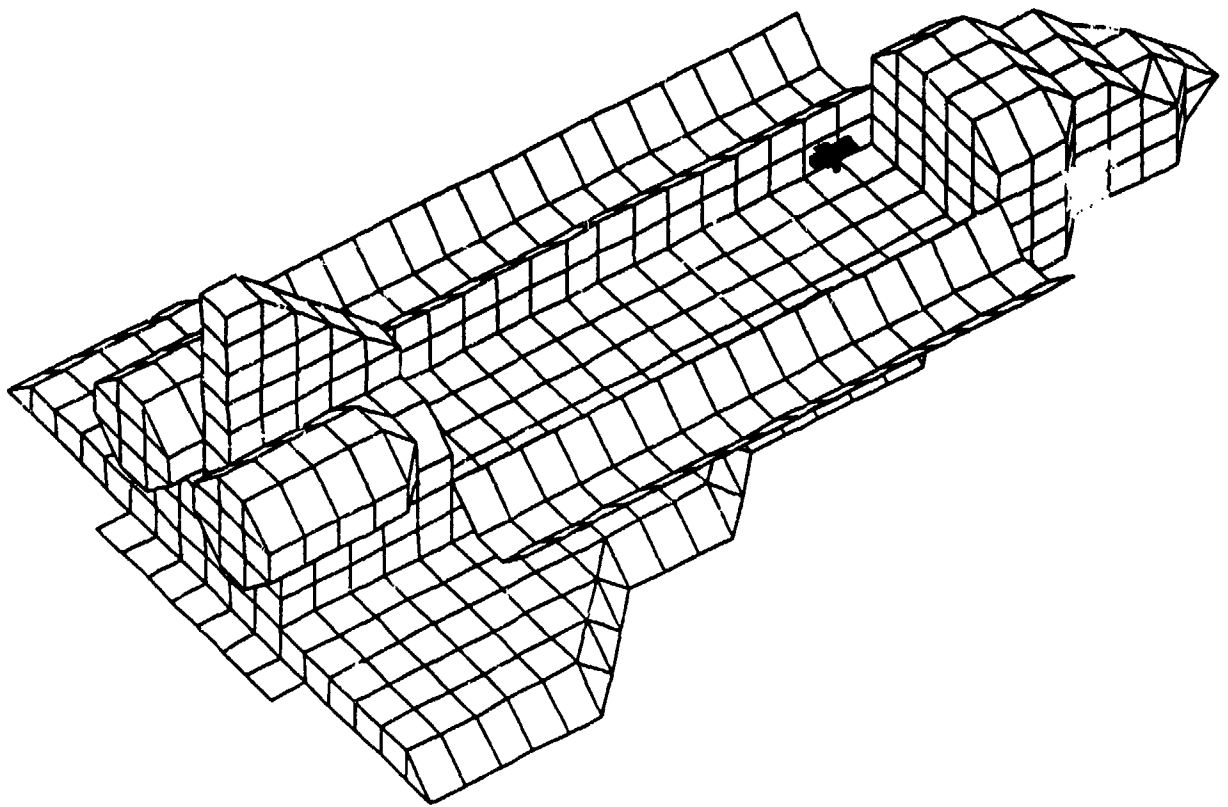
Figure 2. POLAR and NASCAP Model of EMU.

Figure 3. Multi-grid Combined POLAR Model of EMU and Shuttle.

ZMIN = 1.0000E+20 ZMAX = -1.0000E+20 DZ = 0.0000E+00

CONTOUR-LEVELS,VOLTS

-6000.0

-5500.0

-5000.0

-4500.0

-4000.0

-3500.0

-3000.0

-2500.0

-2000.0

-1500.0

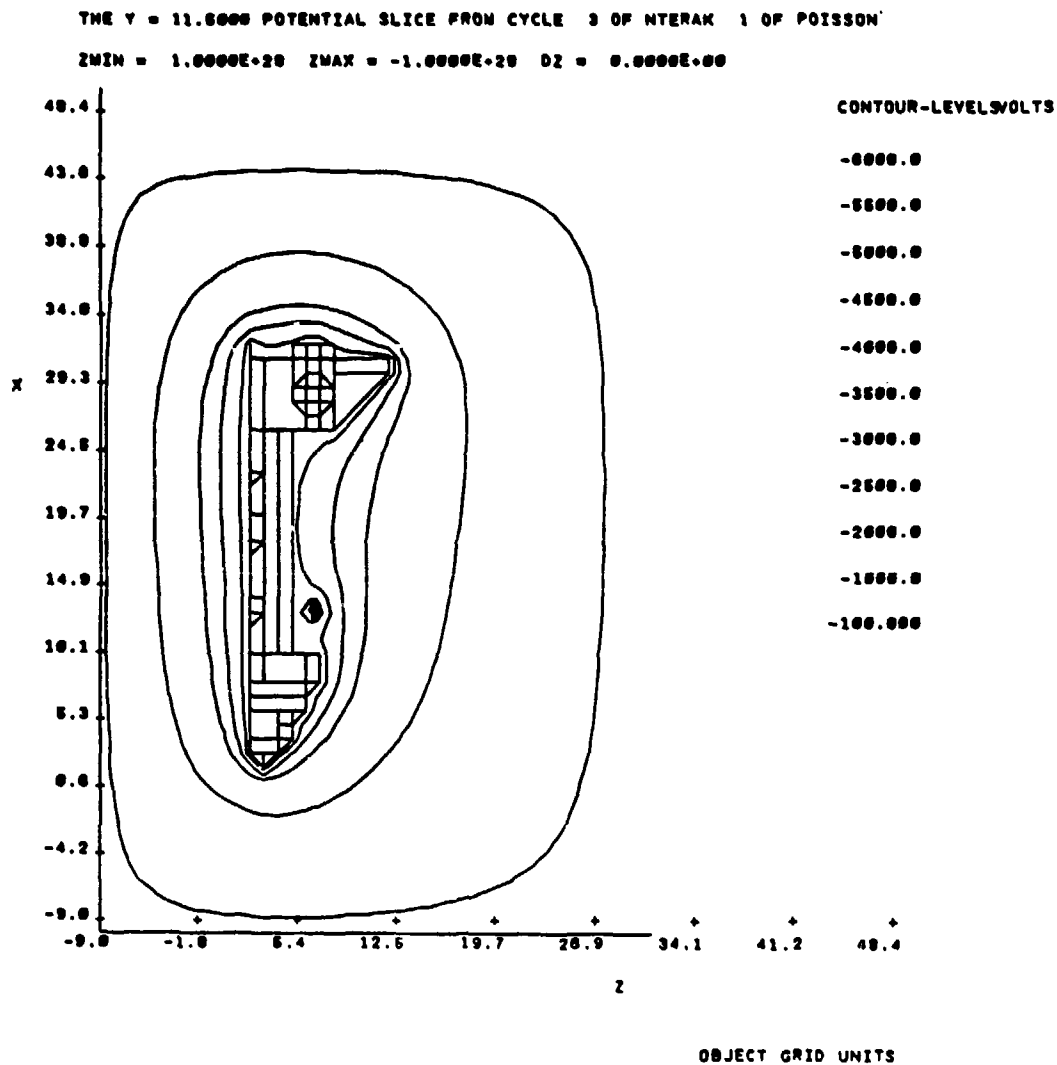-100.000

OBJECT GRID UNITS

Figure 4. Potential Contours of Combined EMU and Shuttle. The Shuttle is at -3290 volts and the EMU predominately -4100 volts but some materials as high as -6000 volts. Note that the EMU affects the potentials only in a region near the EMU.

29

The currents which produce surfacing charging are composed of four parts,

$$J_{total} = J_{auroral} + J_{ion} + J_{sec} + J_{bck}$$

where $J_{auroral}$ and J_{ion} are the auroral electron and collected plasma ion current densities incident on the surface, J_{sec} is the secondary electron current emitted due to ion and electron impact and J_{bck} is the electron backscatter current. The last three currents each contribute a positive current to the surface. Ion induced secondary electrons are ignored in these calculations because of a lack of experimental data on the materials of the EMU and Shuttle. Photo-currents have not been included,hence these calculations can be considered as eclipse calculations.

NASCAP and POLAR use a secondary emission model which is based on the deposition of energy in the material by the incident electron and the ability of the electrons liberated from atoms by this energy to reach the surface of the material. The six parameters needed to model the secondary electron emission are given in the equations below. A detailed description of this model is given in the NASCAP users manual[2].

$$\delta(E_0,\theta) = C \int_0^R \frac{dE_0}{dx} e^{-Ax\cos\theta}$$

$$\frac{dE_0}{dx} = \left(\frac{dR}{dE_0}\right)^{-1} + \left(\frac{d^2R}{dE^2_0}\right)\left(\frac{dR}{dE_0}\right)^{-3} x$$

Where,

$$R = b_1 E_0^{n_1} + b_2 E_2^{n_1}$$

The parameters b_1, n_1 , b_1, n_1 , are entered as material properties in the object definition of NASCAP and POLAR. For convenience, the parameters C and A are computed by the code from the inputed values of the maximum yield value and energy value. The values used for the EMU were determined by fitting ab-initio calculations of secondary electron emission by Ashley et.al.[3] to the NASCAP form given in the above equation. These values are given below by material.

LEXAN

#	PROPERTY	INPUT VALUE	
1	DIELECTRIC CONSTANT	3.50E+00 (NONE)	3.50E+00 (NONE)
2	THICKNESS	1.00E-02 METERS	1.00E-02 MESH
3	CONDUCTIVITY	1.00E-16 MHO/M	1.00E-16 MHO/M
4	ATOMIC NUMBER	5.00E+00 (NONE)	5.00E+00 (NONE)
5	DELTA MAX>COEFF	1.80E+00 (NONE)	2.36E+01 (NONE)
6	E-MAX >DEPTH**-1	2.00E-01 KEV	5.59E-02 ANG-01
7	RANGE	7.15E+01 ANG.	4.29E+01 ANG.
8	EXPONENT> RANGE	6.00E-01 (NONE)	5.13E+02 ANG.
9	RANGE> EXPONENT	2.90E+02 ANG.	6.00E-01 (NONE)
10	EXPONENT	1.77E+00 (NONE)	1.77E+00 (NONE)
11	YIELD FOR 1KEV PROTONS	4.55E-01 (NONE)	4.55E-01 (NONE)
12	MAX DE/DX FOR PROTONS	1.40E+02 KEV	1.40E+02 KEV
13	PHOTOCURRENT	2.00E-05 A/M**2	2.00E-05 A/M**2
14	SURFACE RESISTIVITY	1.00E+16 OHMS	8.85E+04 V-S/Q

WHITE PAINT

#	PROPERTY	INPUT VALUE	
1	DIELECTRIC CONSTANT	3.50E+00 (NONE)	3.50E+00 (NONE)
2	THICKNESS	1.00E-02 METERS	1.00E-02 MESH
3	CONDUCTIVITY	5.90E-14 MHO/M	5.90E-14 MHO/M
4	ATOMIC NUMBER	5.00E+00 (NONE)	5.00E+00 (NONE)
5	DELTA MAX>COEFF	2.10E+00 (NONE)	4.06E+01 (NONE)
6	E-MAX >DEPTH**-1	1.50E-01 KEV	8.74E-02 ANG-01
7	RANGE	7.15E+01 ANG.	4.29E+01 ANG.
8	EXPONENT> RANGE	6.00E-01 (NONE)	5.52E+02 ANG.
9	RANGE> EXPONENT	3.12E+02 ANG.	6.00E-01 (NONE)
10	EXPONENT	1.77E+00 (NONE)	1.77E+00 (NONE)
11	YIELD FOR 1KEV PROTONS	4.55E-01 (NONE)	4.55E-01 (NONE)
12	MAX DE/DX FOR PROTONS	1.40E+02 KEV	1.40E+02 KEV
13	PHOTOCURRENT	2.00E-05 A/M**2	2.00E-05 A/M**2
14	SURFACE RESISTIVITY	1.00E+13 OHMS	8.85E+01 V-S/Q

Table 1. EMU material parameters used in the NASCAP calculations.

```
TEFLON
#    PROPERTY                 INPUT VALUE
1    DIELECTRIC CONSTANT      2.00E+00 (NONE)      2.00E+00 (NONE)
2    THICKNESS                1.00E-02 METERS      1.00E-02 MESH
3    CONDUCTIVITY             1.00E-16 MHO/M       1.00E-16 MHO/M
4    ATOMIC NUMBER            7.00E+00 (NONE)      7.00E+00 (NONE)
5    DELTA MAX>COEFF          2.40E+00 (NONE)      3.00E+01 (NONE)
6    E-MAX >DEPTH**-1         3.00E-01 KEV         1.46E-01 ANG-01
7    RANGE                    4.54E+01 ANG.        1.81E+01 ANG.
8    EXPONENT> RANGE          4.00E-01 (NONE)      1.24E+02 ANG.
9    RANGE> EXPONENT          7.00E+01 ANG.        4.00E-01 (NONE)
10   EXPONENT                 1.77E+00 (NONE)      1.77E+00 (NONE)
11   YIELD FOR 1KEV PROTONS   4.55E-01 (NONE)      4.55E-01 (NONE)
12   MAX DE/DX FOR PROTONS    1.40E+02 KEV         1.40E+02 KEV
13   PHOTOCURRENT             2.00E-05 A/M**2      2.00E-05 A/M**2
14   SURFACE RESISTIVITY      1.00E+16 OHMS        8.85E+04 V-S/Q
```

```
ALUMINUM
#    PROPERTY                 INPUT VALUE
1    DIELECTRIC CONSTANT      1.00E+00 (NONE)      1.00E+00 (NONE)
2    THICKNESS                1.00E-03 METERS      1.00E-03 MESH
3    CONDUCTIVITY             -1.00E+00 MHO/M      -1.00E+00 MHO/M
4    ATOMIC NUMBER            1.30E+01 (NONE)      1.30E+01 (NONE)
5    DELTA MAX>COEFF          9.70E-01 (NONE)      9.18E+00 (NONE)
6    E-MAX >DEPTH**-1         3.00E-01 KEV         3.00E-02 ANG-01
7    RANGE                    1.54E+02 ANG.        1.23E+02 ANG.
8    EXPONENT> RANGE          8.00E-01 (NONE)      3.87E+02 ANG.
9    RANGE> EXPONENT          2.20E+02 ANG.        8.00E-01 (NONE)
10   EXPONENT                 1.76E+00 (NONE)      1.76E+00 (NONE)
11   YIELD FOR 1KEV PROTONS   2.44E-01 (NONE)      2.44E-01 (NONE)
12   MAX DE/DX FOR PROTONS    2.30E+02 KEV         2.30E+02 KEV
13   PHOTOCURRENT             4.00E-05 A/M**2      4.00E-05 A/M**2
14   SURFACE RESISTIVITY      -1.00E+00 OHMS       -8.85E-12 V-S/Q
```

Table 1. Continued

```
KAPT
#     PROPERTY                    INPUT VALUE
1     DIELECTRIC CONSTANT         3.50E+00 (NONE)       3.50E+00 (NONE)
2     THICKNESS                   1.00E-02 METERS       1.00E-02 MESH
3     CONDUCTIVITY                1.00E-16 MHO/M        1.00E-16 MHO/M
4     ATOMIC NUMBER               5.00E+00 (NONE)       5.00E+00 (NONE)
5     DELTA MAX>COEFF             1.80E+00 (NONE)       2.36E+01 (NONE)
6     E-MAX >DEPTH**-1            2.00E-01 KEV          5.59E-02 ANG-01
7     RANGE                       7.15E+01 ANG.         4.29E+01 ANG.
8     EXPONENT> RANGE             6.00E-01 (NONE)       5.13E+02 ANG.
9     RANGE> EXPONENT             2.90E+02 ANG.         6.00E-01 (NONE)
10    EXPONENT                    1.77E+00 (NONE)       1.77E+00 (NONE)
11    YIELD FOR 1KEV PROTONS      4.55E-01 (NONE)       4.55E-01 (NONE)
12    MAX DE/DX FOR PROTONS       1.40E+02 KEV          1.40E+02 KEV
13    PHOTOCURRENT                2.00E-05 A/M**2       2.00E-05 A/M**2
14    SURFACE RESISTIVITY         1.00E+16 OHMS         8.85E+04 V-S/Q
```

Table 1. Continued

The graph below gives the secondary electron emission curves for the five materials of the EMU. Note that Kapton and Lexan have the same secondary electron characteristics. This is because the secondary properties of Lexan were not known. Kapton was chosen as a model of Lexan because they are both insulating plastics.
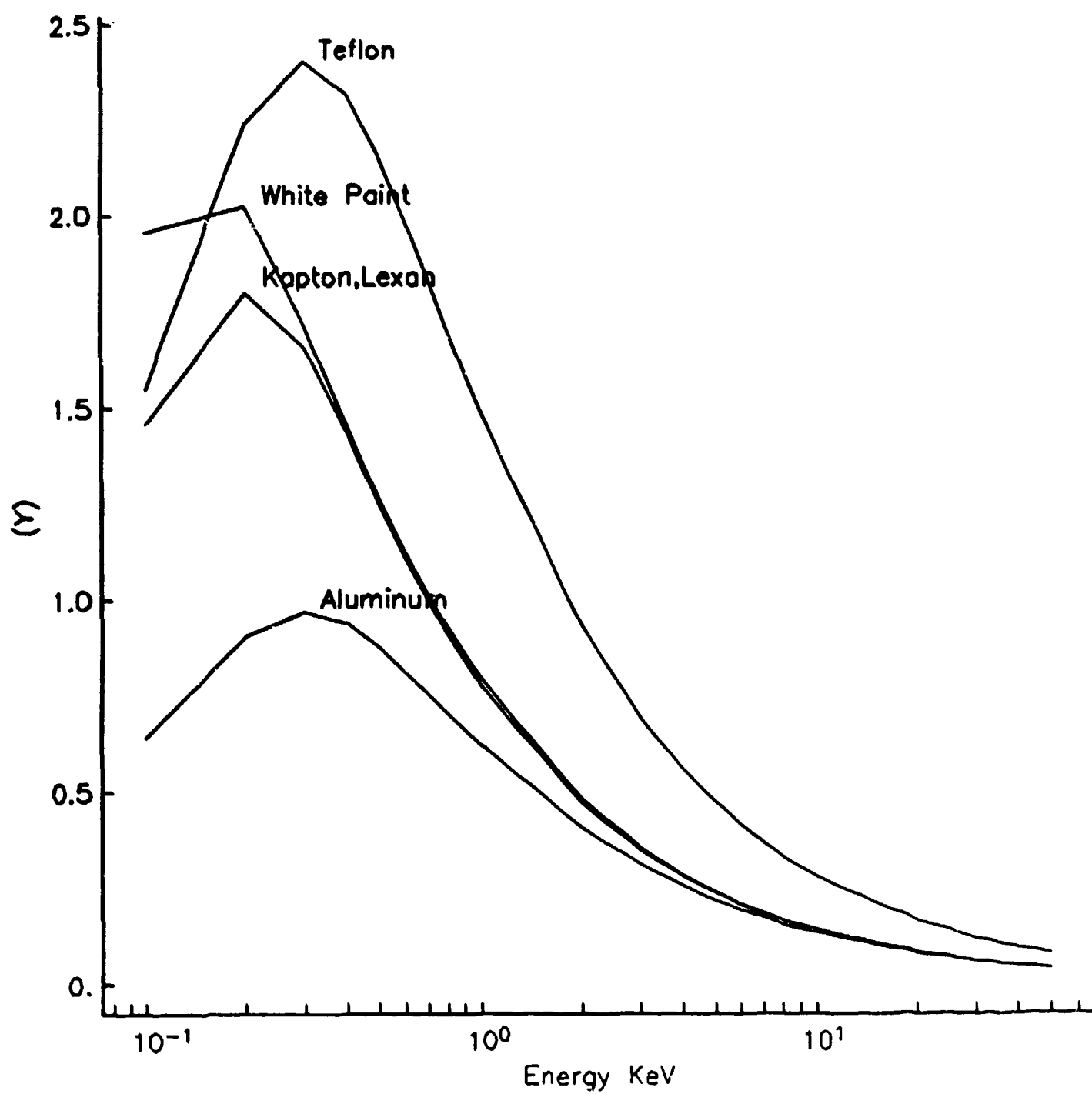
Figure 5. Secondary Electron Emission Coefficients for the EMU Materials.

Backscattered electrons are those emitted from the surface with energies above 50 eV. Their energy distribution is usually peaked close to the primary incident energy and they may be considered as reflected electrons. POLAR and NASCAP employ an empirical representation for the backscattered flux depending only on the atomic number of the material and the incident angle. This form is suggested by experimental data and Monte Carlo data[4], and is

$$\eta(\theta) = e^{-\alpha\cos\theta}$$

where

$$e^{\alpha} = [log(20E)\Theta(E-.05)\frac{\Theta(1-E)}{log(20)} + \Theta(E-1)][.1e^{\frac{-E}{5}} + 1 - (\frac{2}{e})^{.037Z}]$$

where E is in KeV, Z is the atomic number of the material, and Θ is a step function.

The material properties used to model the shuttle charging are given below.

WHITE SPUTTERED TILES			
#	PROPERTY	INPUT VALUE	
1	DIELECTRIC CONSTANT	2.00E+00 (NONE)	2.00E+00 (NONE)
2	THICKNESS	1.00E-02 METERS	1.00E-02 MESH
3	CONDUCTIVITY	1.00E-16 MHO/M	1.00E-16 MHO/M
4	ATOMIC NUMBER	7.00E+00 (NONE)	7.00E+00 (NONE)
5	DELTA MAX>COEFF	1.60E+00 (NONE)	5.91E+00 (NONE)
6	E-MAX >DEPTH**-1	6.00E-01 KEV	1.34E-02 ANG-01
7	RANGE	4.54E+01 ANG.	1.81E+01 ANG.
8	EXPONENT> RANGE	4.00E-01 (NONE)	3.24E+02 ANG.
9	RANGE> EXPONENT	2.00E+02 ANG.	4.00E-01 (NONE)
10	EXPONENT	1.62E+00 (NONE)	1.62E+00 (NONE)
11	YIELD FOR 1KEV PROTONS	4.55E-01 (NONE)	4.55E-01 (NONE)
12	MAX DE/DX FOR PROTONS	1.40E+02 KEV	1.40E+02 KEV
13	PHOTOCURRENT	2.00E-05 A/M**2	2.00E-05 A/M**2
14	SURFACE RESISTIVITY	1.00E+16 OHMS	8.85E+04 V-S/Q

Table 2. Material properties for White Sputtered tiles.

Parameters 5 through 10 in the table above were chosen to fit the measured secondary emission coefficients for the shuttle white tiles as measured by Yang et.al.[5] Data for sputtered tiles was taken because shuttle tiles are most certainly sputtered by Oxygen bombardment in the orbit. The secondary electron emission curve for this material is given in figure 6. The triangles show the experimental values of Yang et.al.
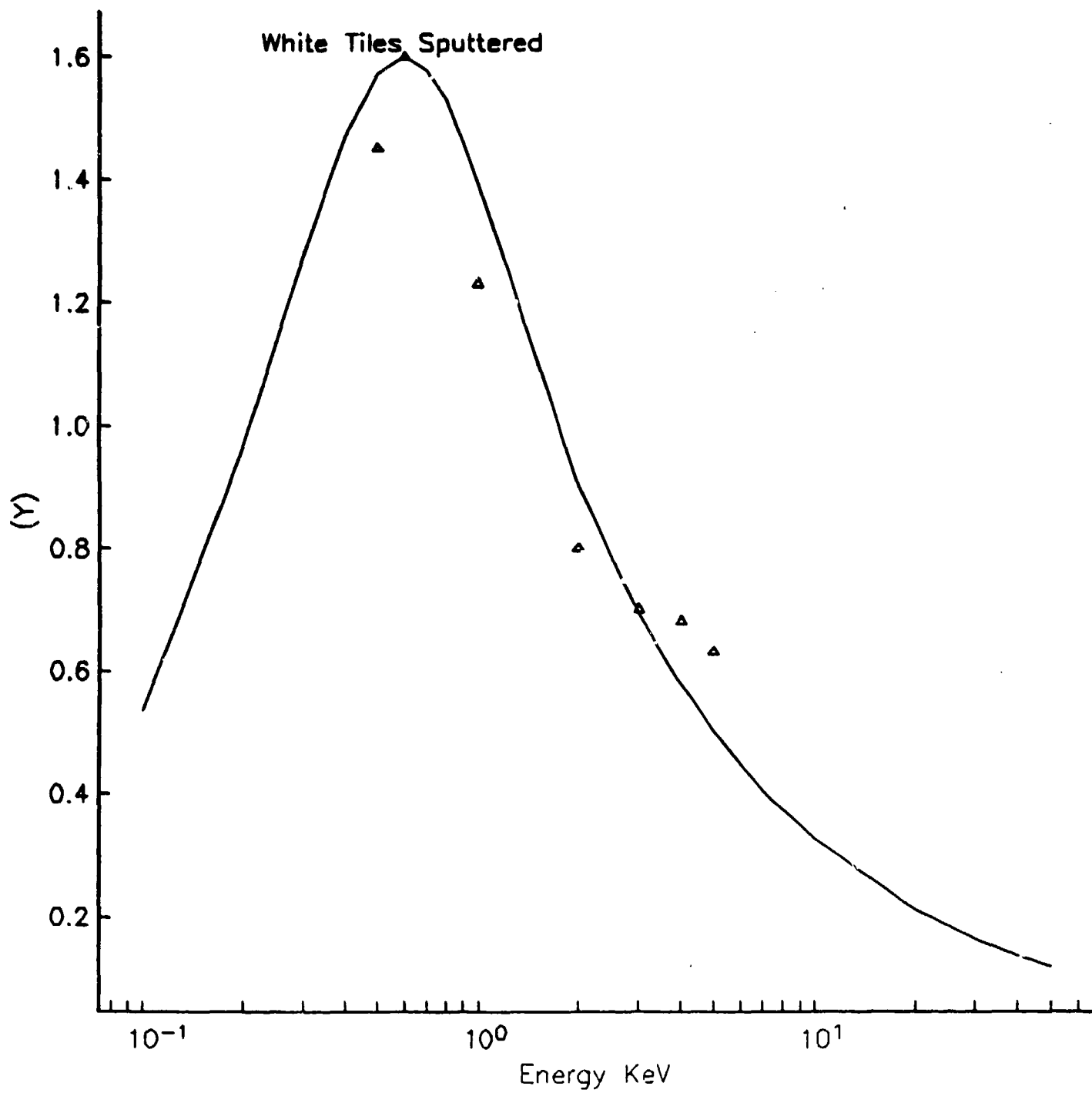
Figure 6.   Secondary Electron Emission Coefficient for the White Sputtered
Tiles.

An area which needs further investigation is the effect of secondary electrons generated by ion impact. Although NASCAP and POLAR account for this positive surface current, the models in the code rely on experimental data which is not accurately known. A preliminary examination of recent data suggests that ion generated secondaries can be a substantial portion of the positive current to the surface for a shuttle size object in the environments seen by the DMSP satellites F6 and F7. This is based on rough estimates for the ion produce secondaries for aluminum taken from a recent publication by Alonso et.al.[6] and should be considered tentative. Increased ion generated secondaries would decrease the shuttle charging potentials over the values calculated in this analysis, however shuttle charging of at least a thousand volts is still expected and differential charging ratios predicted will still be qualitatively correct.
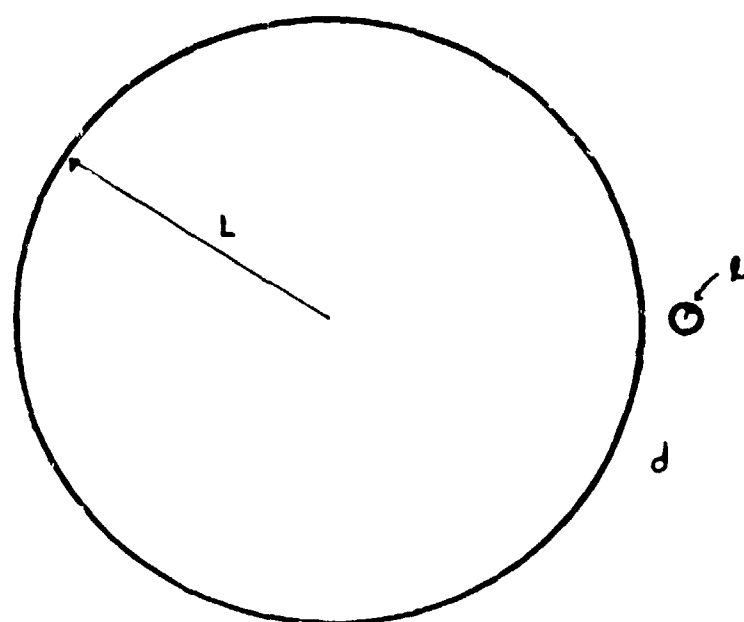
Figure 7. Large and Small Object Coupled Charging.

Differential Voltages and Charging

In this section we will obtain an estimate of the differential charging induced on an EMU performing EVA in the wake of the orbiter. The physical situation to be investigated is therefore a very small object (an EMU of about .5m in radius) near a very large object (an orbiter of about 15m in radius). This is shown in the POLAR code plot, figure 2. As will be shown, the electric fields a few meters from the EMU are determined by the orbiter potential. The ion collection situation for the EMU is thus similar to a probe in a monoenergetic ion beam where the beam energy is the spacecraft potential. If the EMU's material properties are similar to the nearby orbiter then the EMU will charge to the shuttle potential and will collect an ion flux equal to that of the orbiter. However, if the EMU's material surface secondary and backscatter properties are different, then to reach current equilibrium the EMU must charge to a potential different from the shuttle. This will increase or decrease the collected ion flux. As will be shown, a fractional change in differential potential between the orbiter and the EMU is needed to cause a corresponding fractional change in the collected current. Because differences in secondary properties between different materials can cause net collected current to vary by 50 to 75 percent, differential charging of the EMU in the wake of the orbiter can be expected to be on the same scale as the average orbiter charging.

Local Electric Fields

In this section we will estimate the magnitude of the electric field perturbations caused by a small object in the vicinity of a much larger charged object. The situation is depicted in Figure 7. The large sphere represents the orbiter and the small sphere represents the EMU.

Let L be the radius of the large sphere, l the radius of the small sphere and d their separation. The potential of the large sphere is Φ and the smaller sphere differs from this potential by $\Delta\Phi$. The region we are investigating is L >> d >> l and $\Phi = \Delta\Phi$. The crossover point, r, where an ion becomes influenced by the differential potential can be estimated as the point where the electric field from the differential potential equals the electric field from the large sphere. This electric field is due to the potential of the charged large sphere (orbiter) and is given by,

$$E_L = \Phi \frac{L}{(r+L)^2}$$

where r is measured from the surface of the large sphere. Similarly the differential electric field due to the small sphere being at a different potential than

41

the larger sphere can be estimated as

$$E_l = \Delta \Phi \frac{l}{(r-d)^2}$$

As shown in Figure 7, r is the distance from the surface of the larger sphere and taken on a radius which passes through the centers of both spheres. This gives an upper bound on the strength of the field due to the differential charging because the dipole nature of the fields is being ignored and its inclusion would result in a faster drop in the differential voltage field.

This gives for the crossover distance in the limit L >>d >> l,

$$r = \frac{\Delta \Phi}{\Phi} \sqrt{Ll}$$

$$r \rightarrow \sqrt{Ll}$$

Using values for L and l corresponding to an orbiter and an EMU, i.e.,

$$L = 15 meters$$

$$l = .5 meters,$$

we obtain that for the extreme case where the differential charging equals the potential of the orbiter, $\Delta \Phi = \Phi$ that at distances greater than 3 meters from the EMU, the collected ions will not be influenced by the EMU. At this distance from the EMU and the orbiter the space potential is approximately the orbiter potential, ie.

$$v(r) = \phi \frac{L}{(r+L)} = \phi$$

since,

$$\frac{r}{L} \ll 1.$$

Differential Current Collection

We have shown that a EMU charged to a potential $\Delta \Phi$ different from a nearby large orbiter disturbs the local electric fields only a few meters from the EMU. Because, as shown above, the space potential at the crossover region is approximately the orbiter potential, we can estimate the current collected by the EMU using the following;

1) The presence of the large shuttle creates an environment for the EMU consisting of a mono-energetic beam of ions with energy equal to the orbiter potential. This is because the ions are accelerated to the orbiter potential before they are

42

substantially effected by the EMU electric fields, as discussed above.

2)Ion collection by the small EMU in the wake will be orbit limited, with a current density for surfaces at the orbiter potential the same as the average orbiter ion current density. This is because a small probe in a ion beam collects according to orbit limited theory.

The ion collection is then given by,

$$J(\Delta\Phi) = J_o(1 + \frac{\Delta\Phi}{\Phi})$$

Hence, once we have determined the charging of the orbiter to get Φ we can in a second calculation, using the formulation discussed above, determine the ion environment at the EMU, and from this the EMU charging. This last step can be approximated using MATCHG to estimate ΔJ, the variation in charging currents due to surface secondary and backscatter differences, which using the above equation then would give the differential voltages, $\Delta\Phi$, needed to produce these variations. A more accurate NASCAP calculation can be performed using the effective ion environment the shuttle would produce. These two approaches will be presented in sections V and VI.

IV. POLAR Code Calculations

The POLAR code was used to determine the coarse charging that an orbiter EMU pair would produce in an auroral charging environment. The model used for the calculations is shown if figure 8. Although this is a crude model of the orbiter, the over all size and shape is similar. The material covering the model has secondary properties equivalent to the shuttle white tile material and a small patch on the wake side is made of teflon to simulate the EMU.

The auroral environment used in the POLAR calculations was taken from the fits to the observed DMSP environments given by Gussenhoven et. al. This was 10.1 KeV, for the auroral electron temperature and $3.9/cm^3$ for the density. The cold ion density was taken to be the observed density of $125/cm^3$.

POLAR code calculations were performed for a range of voltages from -1000 volts to -4500 volts. From these calculations a current verses voltage relationship was determined. A plot of I Vs V for the shuttle shown in Figure 9. Also shown on this figure is the net electron current to the shuttle surface. This current is composed of three terms

$$I_{net} = I_{incident} + I_{secondary} + I_{backscatter}$$

The last two terms in the above equation contribute a positive current. The point of intersection of the two curves is the steady state charging potential of the shuttle. For reasons discussed in section III, ion generated secondaries have been neglected in this calculation. From Figure 9 it is clear that shuttle charging is reduced as ion generated secondary emission is increased. Figure 10 shows contour plots for the charged shuttle at the -3290 volt equilibrium potential.
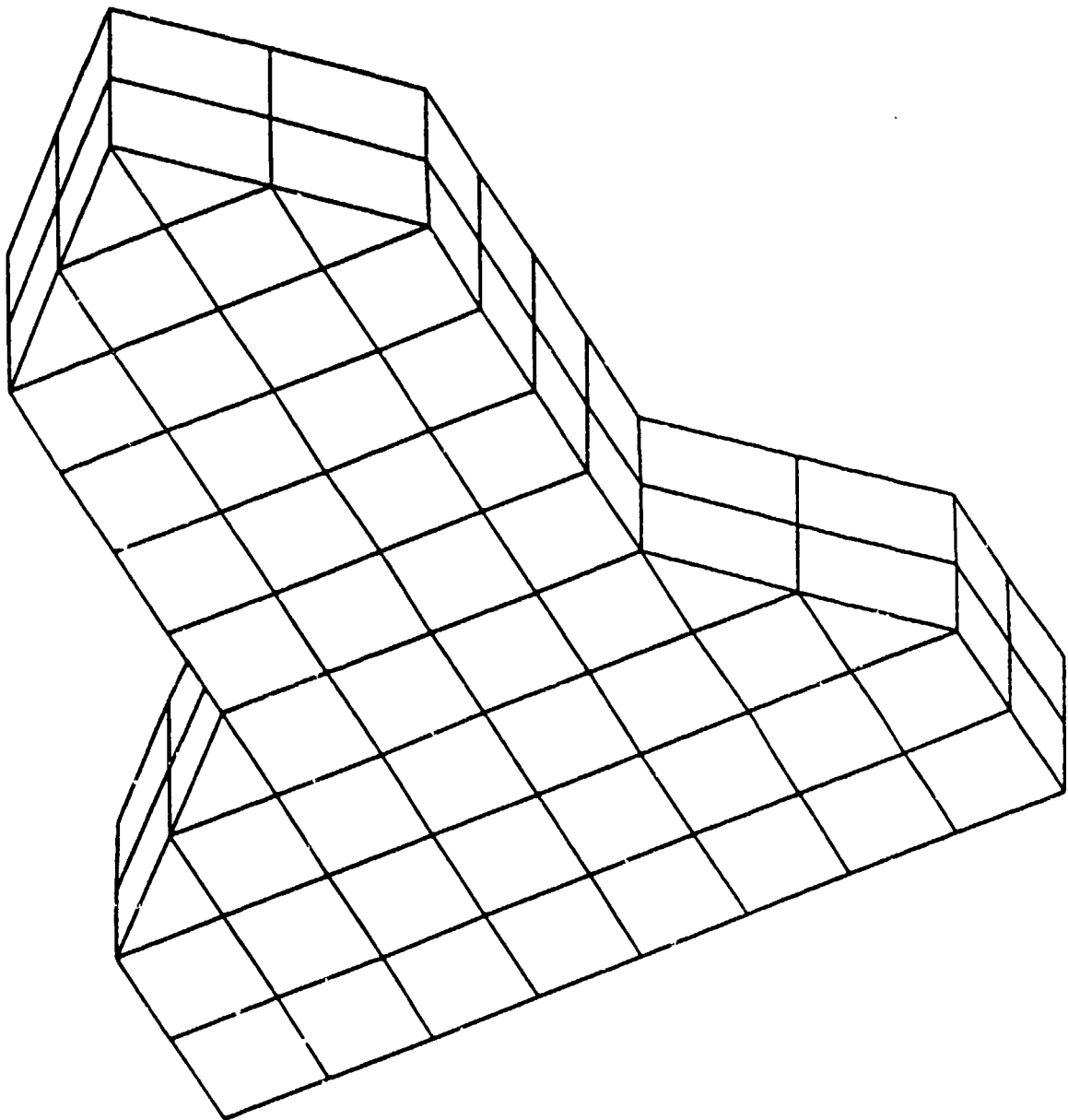
Figure 8. POLAR Model of Shuttle Used for the I vs V Determination.

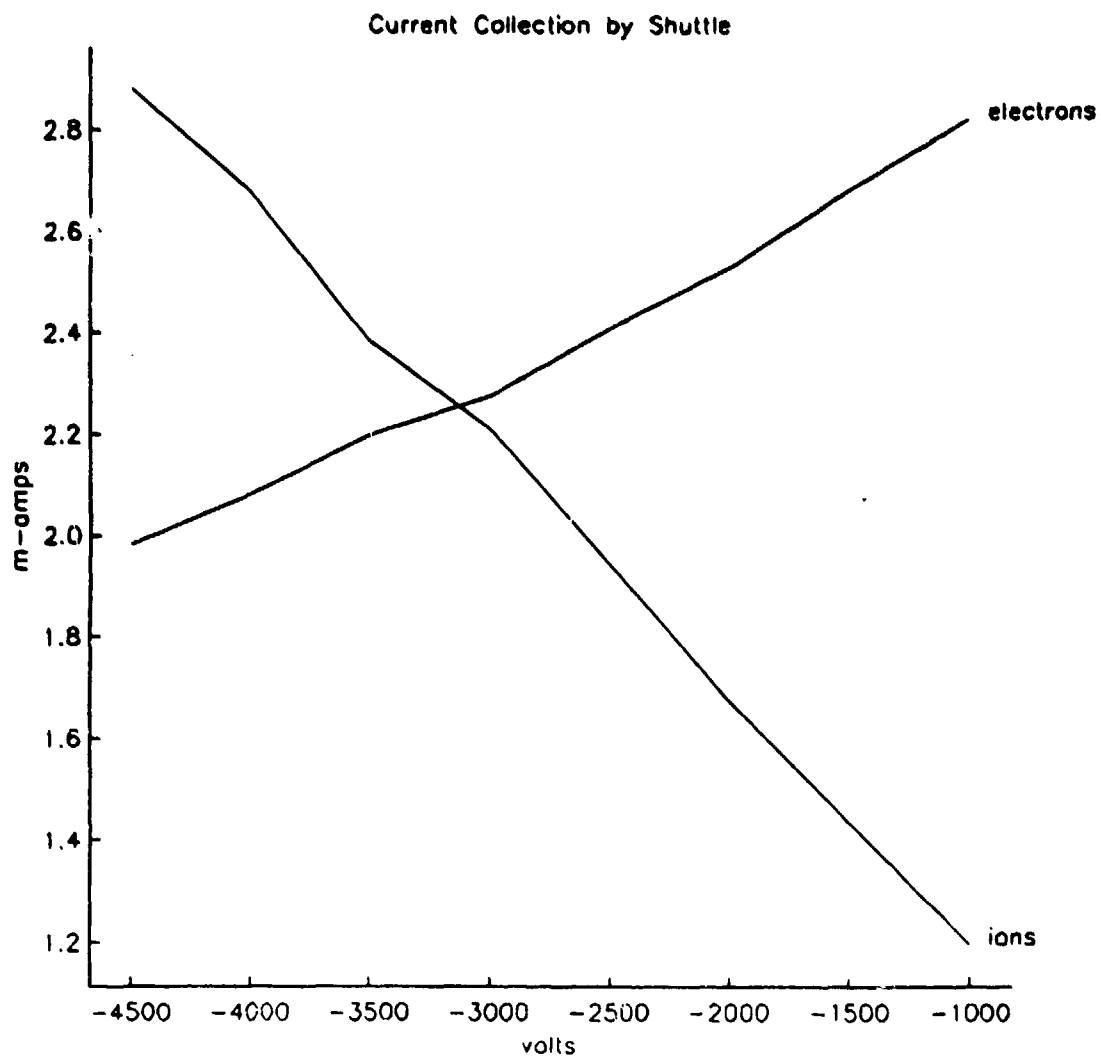Current Collection by Shuttle

Figure 9.   POLAR Calculations of the Shuttle Current Collection vs
            Voltage. The curve labeled "electrons" is the net current of
            electrons to the surface including backscatter and secondary.
            The intersection point is the steady state charging potential of
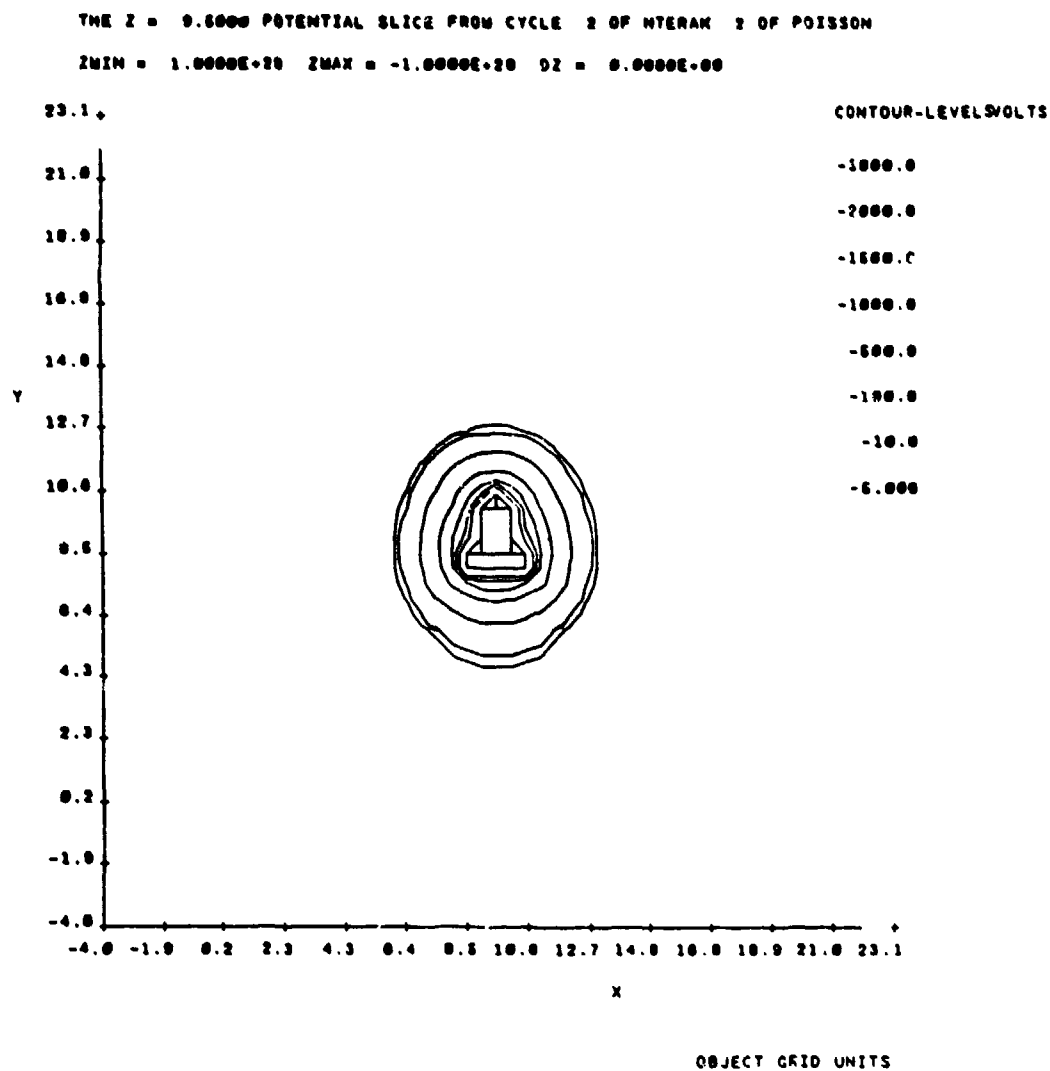   the shuttle.

46

CONTOUR-LEVELS/VOLTS

-3000.0

-2000.0

-1500.C

-1000.0

-500.0

-190.0

-10.0

-5.000

OBJECT GRID UNITS

Figure 10.   POLAR Potential Calculation of the Charged Shuttle

47

V. MATCI ; Calculations of EMU Charging

The environment used in the MATCHG calculations was identical to that for the POLAR calculations and discussed in section IV. The hot electron spectrum was a single Maxwellian with temperature 10.1 KeV and a density of $3.9/cm^3$. The ion temperature and density are chosen so that the slope of the ion current collection verses voltage is the correct orbit limited value derived in section III. This turned out to be $.52/cm^3$. The temperature is chosen .0048 KeV corresponding to the ram energy of ambient oxygen ions. With this choice of plasma temperature and density MATCHG will correctly model the orbit limited charging of the materials.

Table 2 shows the charging potentials and charging currents for 8 different materials typical of the shuttle and EMU. As is seen, variations of 3000 volts over the EMU and between the EMU and the shuttle are expected due to differences in material secondary and backscatter properties. A summary of the material charging is shown below for the 8 materials.

Material	Net Electron Current	Potential	
Kapton	2.86 uA/M**2	-6290 volts	
White Tiles (sputtered)	1.15	-3290	*
Teflon	1.56	-4090	
Aquadag	2.67	-6000	*
White Non Conducting Paint	4.04	-2700	
Gold	0.	.4	*
Alum	2.20	-6800	
*Not a suit material.			

Table 2. Charging potentials for selected materials. The column
labeled Net Charging Current is sum of the incident electron
current, secondaries and backscatter.

VI. NASCAP Calculations

In this section we will present two calculations of the differential charging expected on the EMU in the wake of a Polar orbiting shuttle. NASCAP calculations were performed using the EMU model shown in Figure 2. The material properties, such as secondary and backscatter emissions, were chosen to closely model those of the actual EMU. Figures 11a through 11f show the EMU material construction as modeled in the POLAR and NASCAP calculations. As in the MATCHG calculations, the hot electron temperature and density where take from fits to DMSP data given by Gussenhoven. The cold ion environment was chosen similar to the MATCHG calculations where the temperature is taken to be low to simulate the mono-energetic nature of the charging environment of the EMU, and the density is chosen to give the proper orbit limited current verses voltage characteristic.

The results of the NASCAP calculations are given in Table 3. Reading down the columns shows the convergence of the NASCAP charging calculation indicating that the final few iterations are well converged for all but the ground conductor. For the aluminum components and the suit ground, the differential charging time scale is tens of seconds which was longer than the NASCAP calculations were run. Figure 13 shows the potentials of the suit ground (ALUMINUM) and the kapton gloves as a function of time. The aluminum is still charging while the kapton has reached the current balance predicted by the MATCHG calculations. This long charging time scale results from the relatively small current collection area for the suit ground. The charging time scale for the suit ground can be estimated using the incident electron current to the aluminum patches and the capacitance between the suit surface and the underlying ground.

$$\frac{dV_{ground}}{dt} = \frac{I_g}{C_g}$$

$$= -J_{elec}\frac{A_{alum}}{C_g}$$

$$= -\frac{dJ_{elec}}{\epsilon_0}\frac{A_{alum}}{A_{suit}}$$

where $C_g = \epsilon_0\frac{A_{suit}}{d}$ is the suit capacitance, J_{elec} is the net electron current to the surface, and $A_{alum} = .07m^2$ is the exposed area of suit ground (aluminum) and $A_{suit} = 5.8m^2$ is the suit surface area. From the MATCHG calculations this gives $J_{elec} = -2.2\mu\frac{A}{m^2}$ a charging rate of $\frac{dV}{dt} = -26\frac{volts}{sec}$ in agreement with the $-16\frac{volts}{sec}$ from Table 3. Over 100 seconds are required to reach the -6800 volts expected from the MATCHG calculations The MATCHG calculations showed that the aluminum surfaces should charge to more than 6000 volts negative given sufficient

49

time. Figures 14 and 15 show potential contours about the EMU for this charging calculation. As seen, potentials on the face plate of the astronaut are thousands of volts higher than on the suit material of the EMU.

Differences between MATCHG and NASCAP result from NASCAPs proper inclusion of three dimensional effects. Current balance is effected by leakage currents to underlying conductors and surface conductivity. In addition, adjacent surfaces which are charging differently due to secondary property differences, can effect each other's charging characteristics becuase of electric field effects on secondary emission.

| POTENTIAL IN KILO-VOLTS							
TIME	B	C	D	E	F	G	H
4.1E-03	-.094	-.094	-.095	-.093	-.092	-.095	-.68
6.7E-03	-1.39	-1.39	-1.39	-1.39	-1.38	-1.39	-1.36
1.4E-02	-2.06	-2.06	-2.06	-2.06	-2.06	-2.06	-2.04
2.1E-02	-2.73	-2.73	-2.73	-2.72	-2.72	-2.73	-2.67
3.1E-02	-3.31	-3.31	-3.31	-3.29	-3.29	-3.31	-3.24
1.3E-01	-4.23	-4.23	-4.23	-4.18	-4.16	-4.23	-4.09
2.3E-01	-4.41	-4.41	-4.41	-4.27	-4.39	-4.41	-4.21
3.3E-01	-4.50	-4.50	-4.50	-4.30	-4.32	-4.50	-4.24
4.3E-01	-4.55	-4.55	-4.55	-4.30	-4.32	-4.56	-4.24
5.3E-01	-4.60	-4.60	-4.60	-4.29	-4.33	-4.61	-4.23
6.3E-01	-4.65	-4.65	-4.65	-4.28	-4.33	-4.65	-4.23
7.3E-01	-4.70	-4.70	-4.70	-4.28	-4.33	-4.70	-4.22
8.3E-01	-4.75	-4.75	-4.74	-4.27	-4.33	-4.75	-4.22
9.3E-01	-4.79	-4.79	-4.79	-4.27	-4.33	-4.80	-4.22
1.0E+00	-4.84	-4.84	-4.83	-4.26	-4.33	-4.84	-4.22
1.3E+00	-4.94	-4.94	-4.93	-4.25	-4.34	-4.95	-4.21
1.5E+00	-5.04	-5.04	-5.03	-4.25	-4.35	-5.04	-4.21
1.8E+00	-5.13	-5.13	-5.12	-4.24	-4.35	-5.13	-4.20
2.0E+00	-5.22	-5.22	-5.20	-4.23	-4.36	-5.22	-4.20
2.3E+00	-5.30	-5.30	-5.28	-4.23	-4.36	-5.30	-4.20
2.5E+00	-5.37	-5.37	-5.35	-4.22	-4.37	-5.37	-4.19
2.8E+00	-5.44	-5.44	-5.42	-4.22	-4.38	-5.44	-4.19
3.0E+00	-5.51	-5.50	-5.48	-4.21	-4.38	-5.51	-4.19
3.3E+00	-5.56	-5.56	-5.54	-4.20	-4.39	-5.57	-4.18
3.5E+00	-5.62	-5.62	-5.59	-4.20	-4.39	-5.62	-4.18
3.8E+00	-5.67	-5.67	-5.64	-4.19	-4.40	-5.67	-4.18
4.0E+00	-5.71	-5.71	-5.69	-4.19	-4.40	-5.72	-4.17
4.3E+00	-5.76	-5.76	-5.73	-4.18	-4.40	-5.76	-4.17
4.5E+00	-5.80	-5.80	-5.77	-4.18	-4.41	-5.80	-4.17
4.8E+00	-5.84	-5.84	-5.80	-4.18	-4.41	-5.84	-4.16
5.0E+00	-5.87	-5.87	-5.84	-4.17	-4.41	-5.87	-4.16
5.3E+00	-5.90	-5.90	-5.87	-4.17	-4.42	-5.90	-4.16
5.5E+00	-5.93	-5.93	-5.90	-4.17	-4.42	-5.93	-4.16
5.8E+00	-5.96	-5.96	-5.92	-4.16	-4.42	-5.96	-4.15
6.0E+00	-5.99	-5.99	-5.95	-4.16	-4.43	-5.99	-4.15
6.3E+00	-6.01	-6.01	-5.97	-4.16	-4.43	-6.01	-4.15
6.8E+00	-6.05	-6.05	-6.01	-4.15	-4.44	-6.05	-4.15
7.3E+00	-6.09	-6.09	-6.05	-4.15	-4.44	-6.09	-4.14
7.8E+00	-6.12	-6.12	-6.08	-4.16	-4.45	-6.12	-4.14
8.3E+00	-6.15	-6.15	-6.11	-4.16	-4.45	-6.15	-4.14
8.8E+00	-6.17	-6.17	-6.13	-4.17	-4.46	-6.17	-4.14

Table 3 Results of NASCAP calculation of EMU charging in the near shuttle environment. The letters B,C,D,E,F,G refer to locations on the EMU shown in Figure 12

SURFACE CELL MATERIAL COMPOSITION AS VIEWED FROM THE POSITIVE Y DIRECTION

FOR Y VALUES BETWEEN 1 AND 17

MATERIAL LEGEND

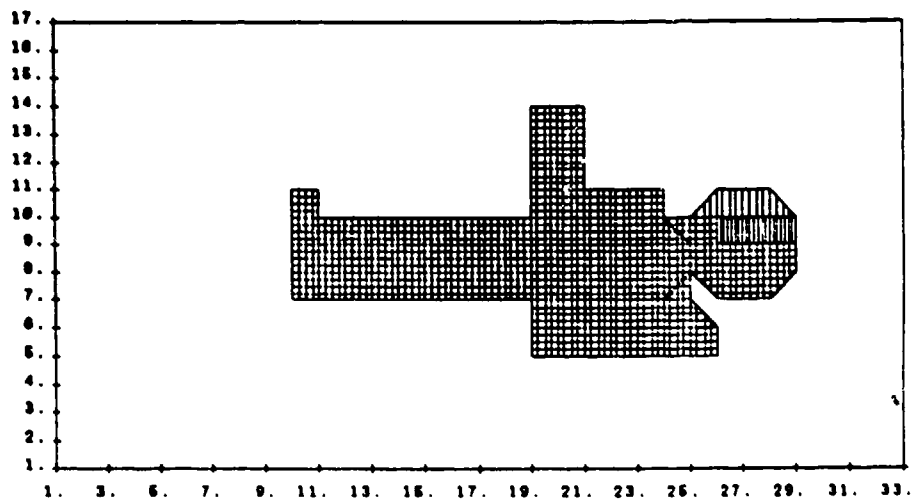2
LORD

3
ALUM

6
TEFL

7
KAPT
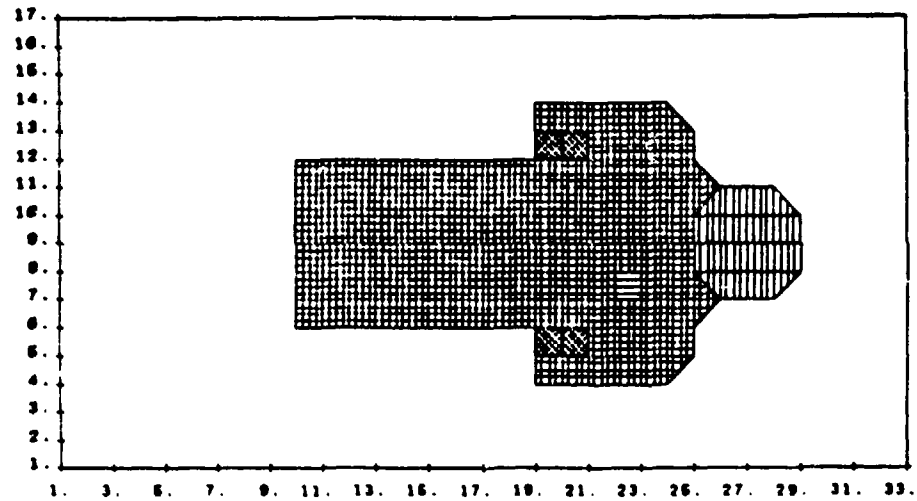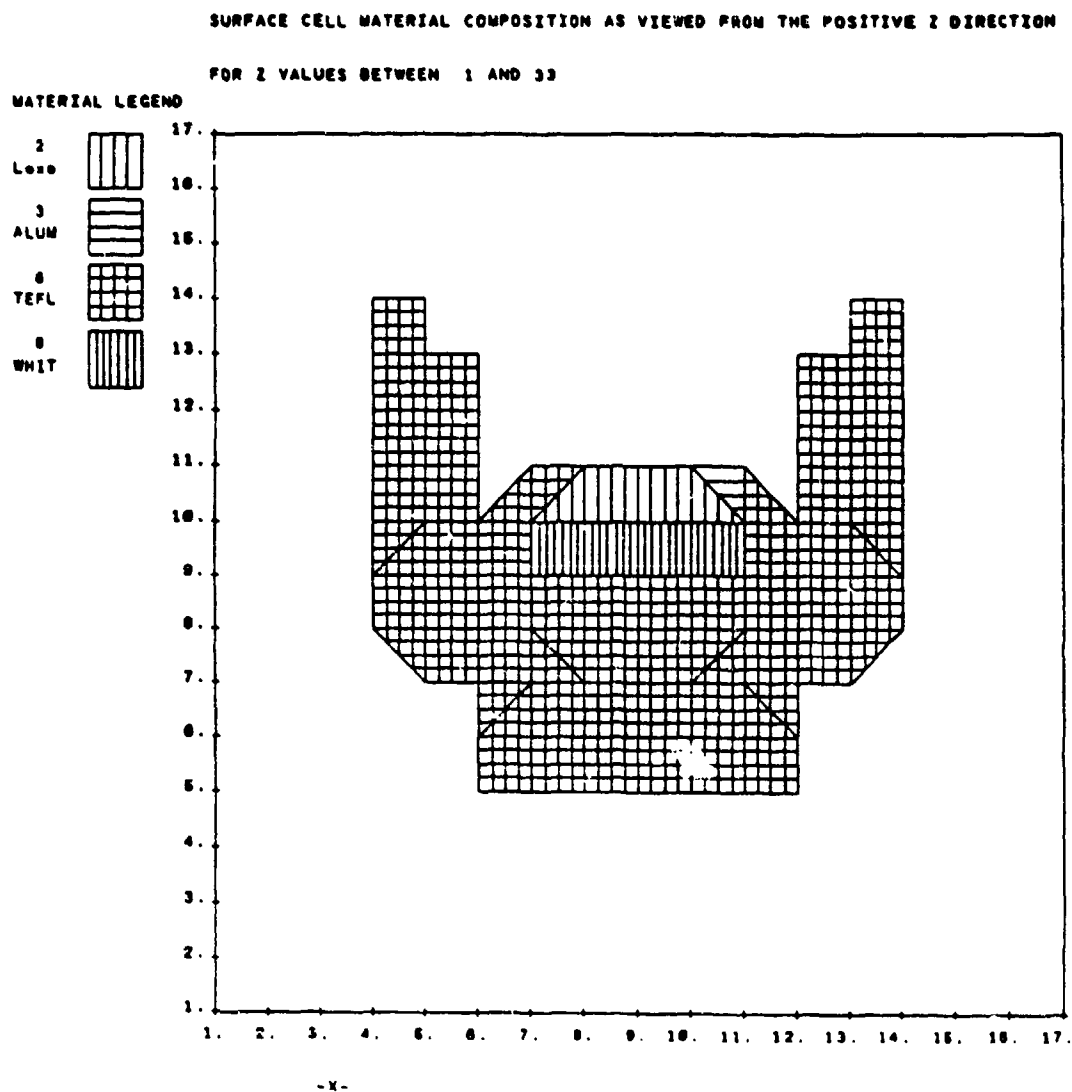
Figure 11. (a) NASCAP Material Plots of the EMU.

SURFACE CELL MATERIAL COMPOSITION AS VIEWED FROM THE NEGATIVE X DIRECTION

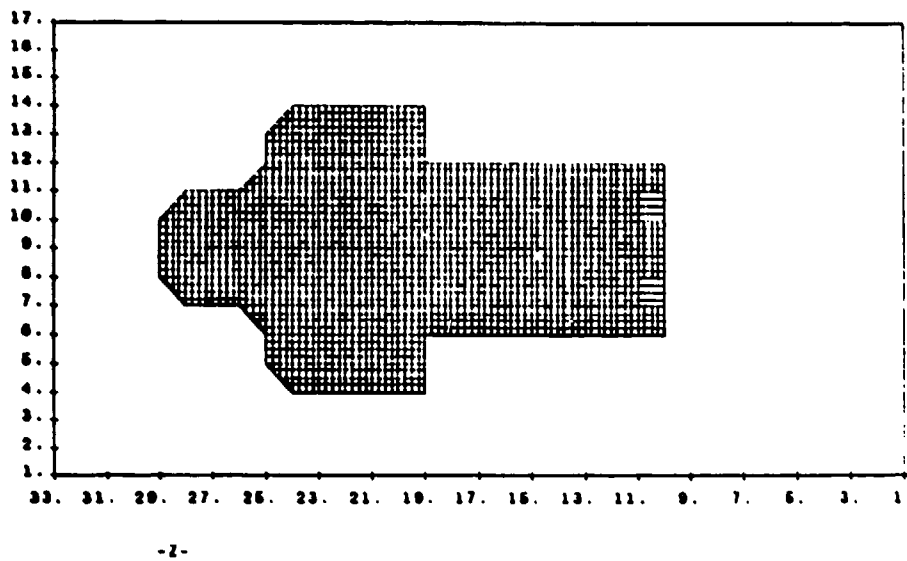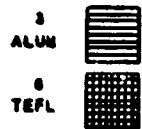FOR X VALUES BETWEEN 1 AND 17

MATERIAL LEGEND

Figure 11. (b) NASCAP Material Plots of the EMU.

53

MATERIAL LEGEND

2
Loxo

3
ALUM

8
TEFL

8
WHIT

-X-

Figure 11.   (c)   NASCAP Material Plots of the EMU.

54

MATERIAL LEGEND

3
ALUM

6
TEFL
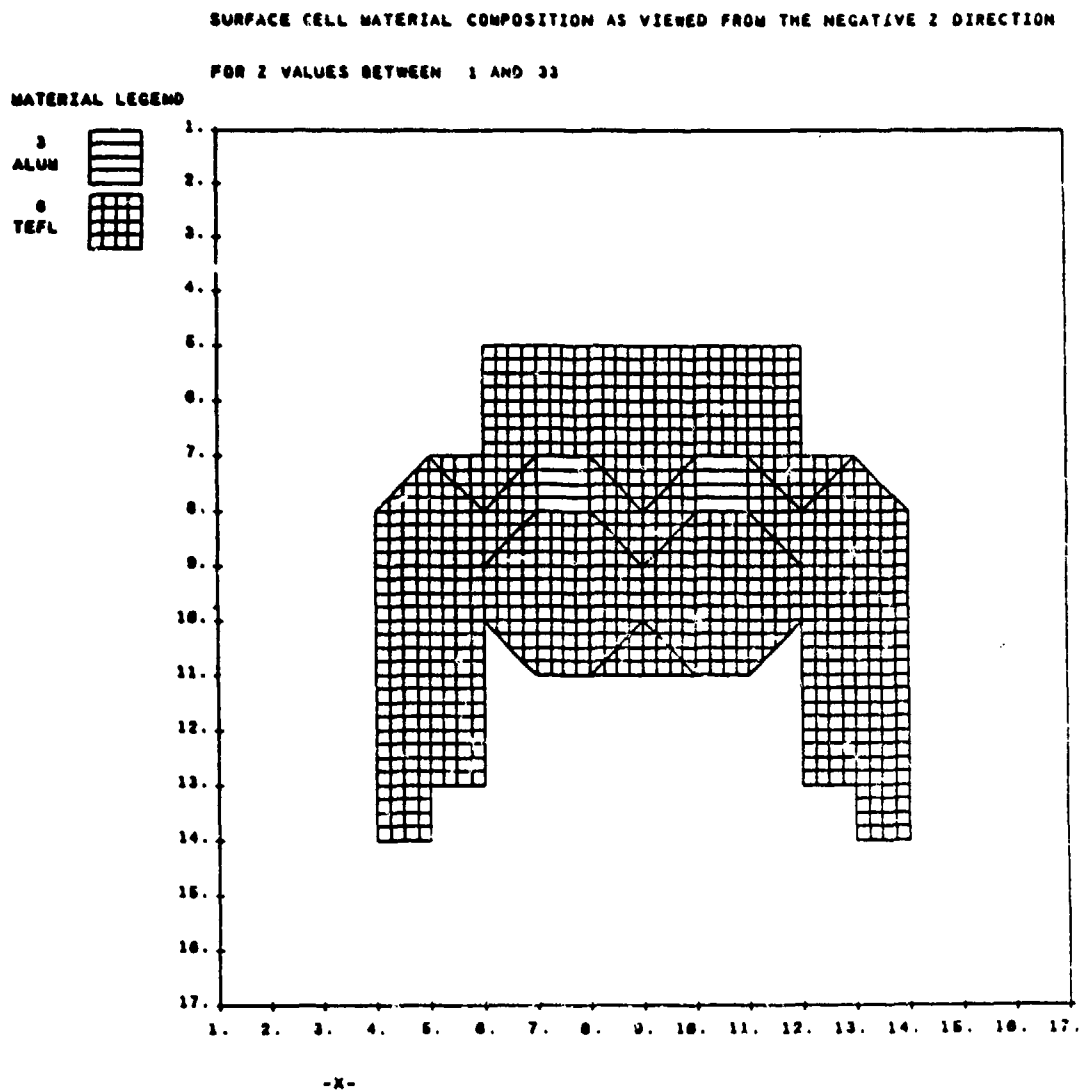
Figure 11. (d) NASCAP Material Plots of the EMU.

SURFACE CELL MATERIAL COMPOSITION AS VIEWED FROM THE POSITIVE X DIRECTION

FOR X VALUES BETWEEN 1 AND 17

MATERIAL LEGEND

2
LOAD

6
TEFL

8
WHIT
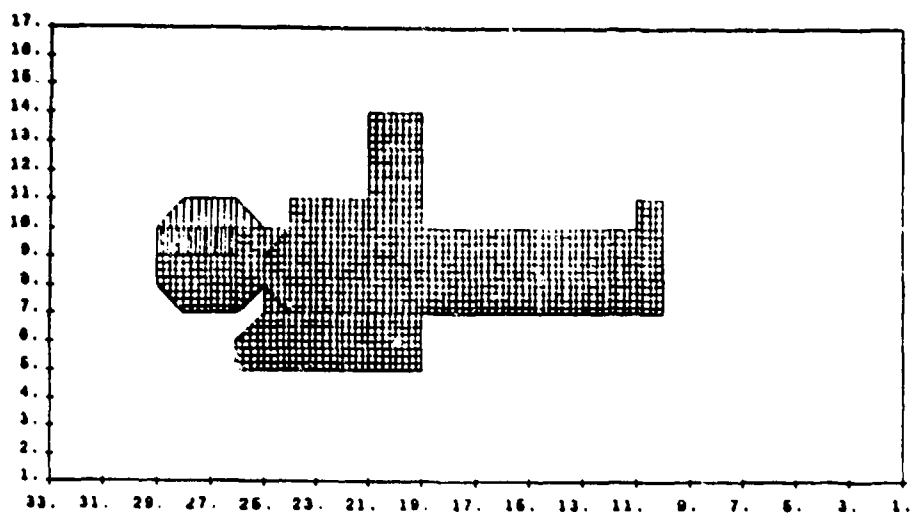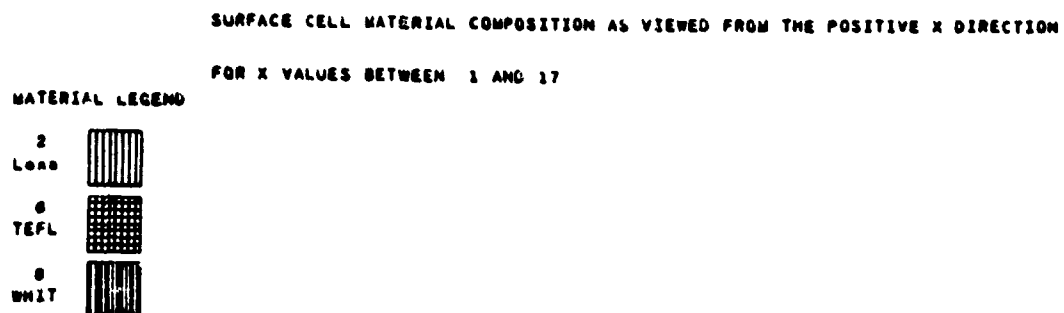
-2-

Figure 11. (e) NASCAP Material Plots of the EMU.

Figure 11. (f) NASCAP Material Plots of the EMU.
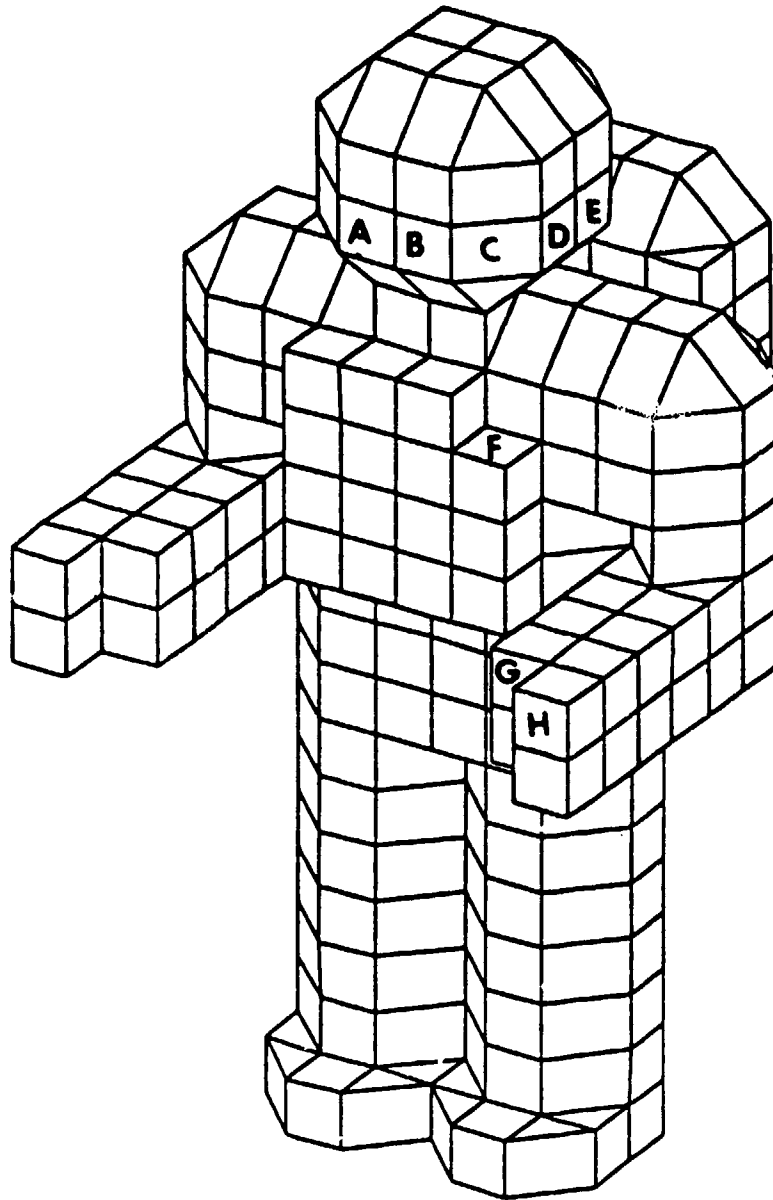
Figure 12.   The Labeled Surfaces B-H Refer to the Time History Shown in
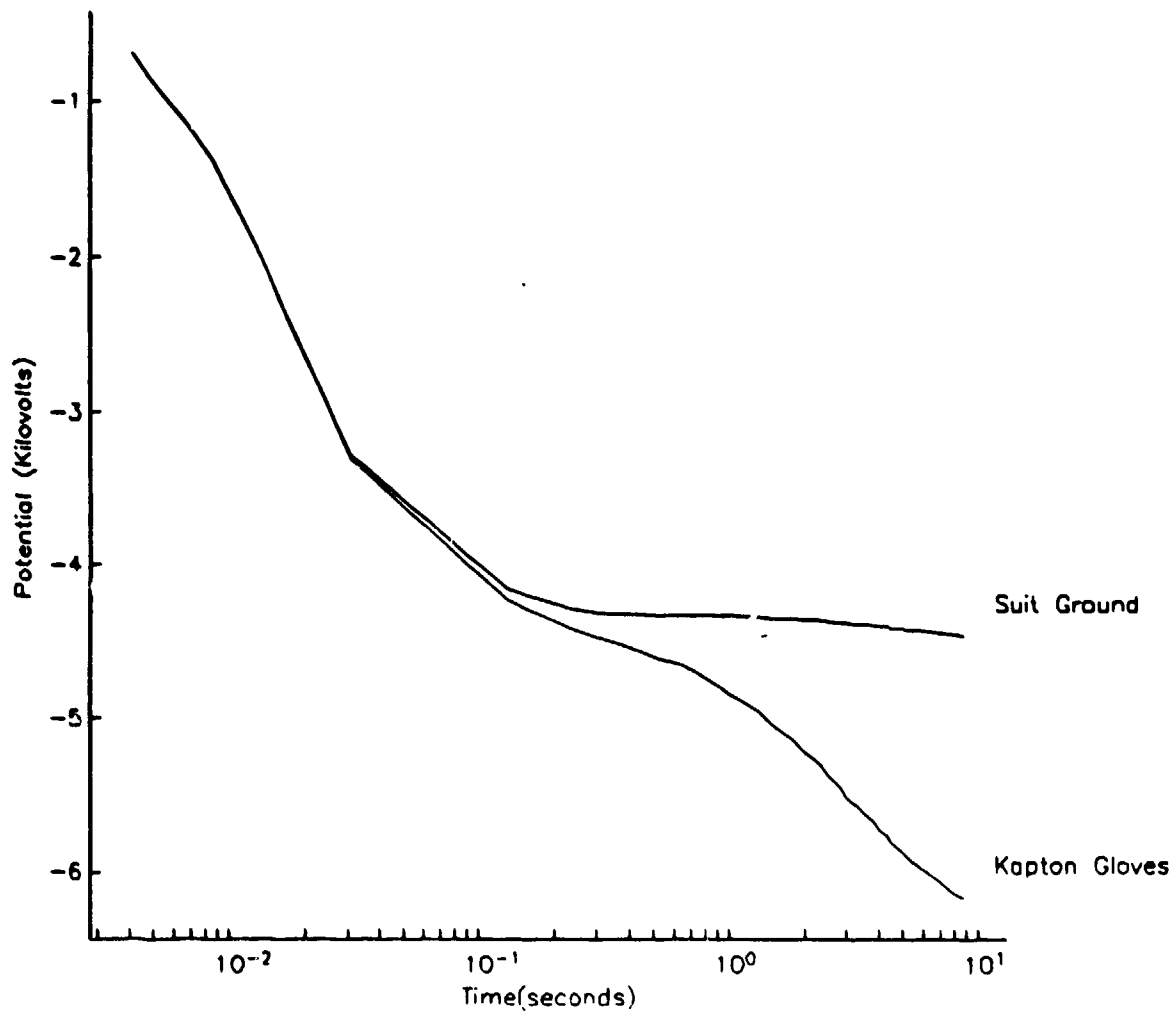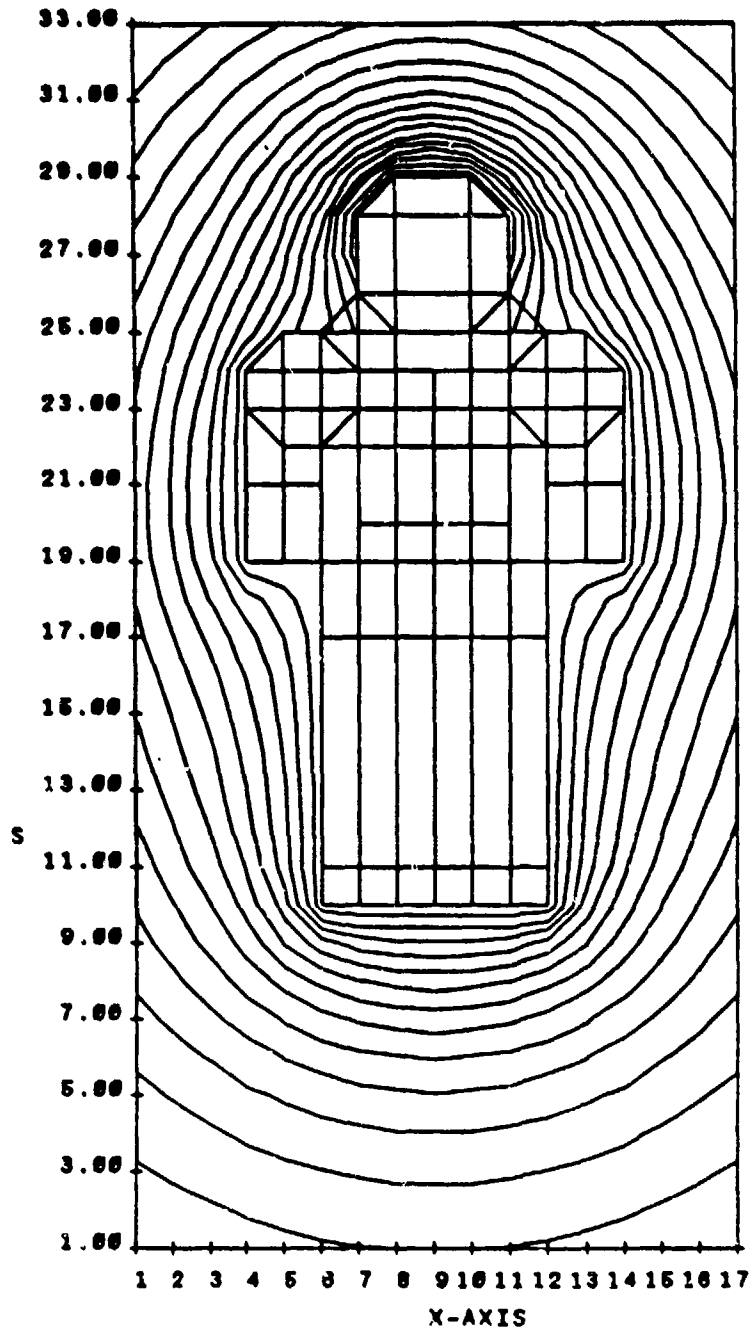Table 3.

58

Figure 13. Time History of Charging of the Suit Ground and Kapton Gloves.

-5.14E+03 < CONTOUR LEVELS < -1.43E+93   AT POTENTIAL INCREMENTS OF DP = 2.00E+02
      1.00 <X< 17.00,   1.00 <Z<   33.00, CUTPLANE OFFSET Y=   9.00

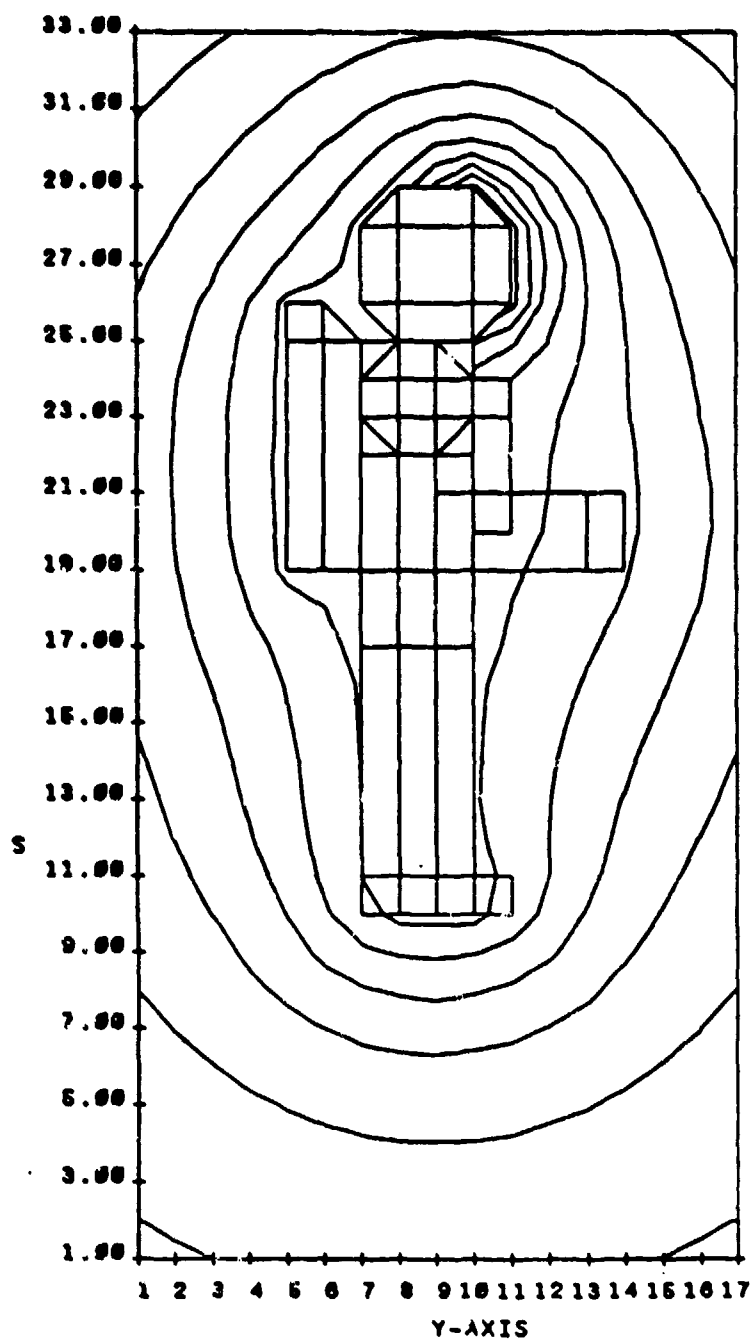Figure 14.   Potential Contours Around Charge EMU.

60

Figure 15.   Potential Contours Around Charge EMU.

VII. Stored Electrical Energy in the EMU

Energy is stored in the EMU through capacitance to infinity and to underlying conductors. The quantity of energy in each of these modes depends on the voltages and capacitances as,

$$E_\infty = \frac{1}{2} C_\infty V^2$$

$$E_{\delta v} = \frac{1}{2} C_g (\delta V)^2$$

where δV is the voltage difference between the suit surface material and the suit ground, where V is the surface voltage relative to infinity, and C_∞ is the capacitance to infinity. These capacitances can be estimated by approximating the EMU as a conducting spherical ball with radius R and covered with teflon of thickness d. The capacitance to infinity can then be determined by the definition of capacitance,

$$Q = CV$$

and the relationship between charge and potential on a sphere,

$$V = \frac{Q}{4\pi\epsilon_0 R}$$

This gives for the capacitance of a sphere,

$$C_\infty = 4\pi\epsilon_0 R$$

$$= 10^2 pF \ (1 meter \ object)$$

The capacitance to the underlying conductor (suit ground) C_g is much larger and can be estimated assuming a parallel plate capacitor of area the surface area of the EMU. The capacitance of a parallel plate capicator is,

$$C_g = k\epsilon_0 \frac{A}{d}$$

where k is the dielectric constant which we will call 1 for these estimates, A is the surface area, and d the thickness of the insulating suit material . For a spherical EMU the surface area is $A = 4\pi R^2$ so the capacitance to suit ground is

$$C_g = 4\pi\epsilon_0 \frac{R^2}{d}$$

which for a 1 meter radius EMU with 1 centimeter of insulating material results in

$$C_g = 10^4 pF$$

Hence $C_g = \frac{R}{d} C_\infty = 100 C_\infty$, so for comparable voltages much more energy is stored

The MATCHG calculations showed that the dominant material, teflon, would charge to approximately -4000 volts and that the face plate material would charge to -6000 volts, and the suit ground to about -6800 volts. Hence, $V_{\infty}=-4000v$ and $\delta V=-1000v$. Using these values E_{∞} and $E_{\delta V}$ can be estimated as,

$$E_{\infty}=1^{-3} Joules$$

$$E_{\delta}=.1 Joules$$

These calculations are upper bounds on the energy involved in a discharge because they assume all the stored charge is transferred in the discharge. In realistic discharges only a fraction of the charge (depending on the geometry and the type of discharge) contributes to the discharge.

These estimates can be improved using the results of the NASCAP calculation. The NASCAP code computes the capacitance to infinity for a three dimensional object as part of its charging algorithm. For the EMU NASCAP gives the effective radius of $R_{eff}=.608M$ thus $C_{\infty}=68pF$, and $E_{\infty}=.310^{-3} Joules$.

Two other important points should be made at this point. First, grounding the astronaut would increase the arcing hazard by fixing the suit ground at the shuttle ground. This would increase δV by a factor of three and hence the stored energy by ten fold. Secondly, The charging of the suit ground happens on time scale which is much slower than the other charging times because of the relatively small amount of exposed ground conductor. Hence, for early times (as seen in the NASCAP charging history shown section VI) the differential voltage, δV is over twice the steady state value of 800-1000 volts.

63

VII. Stored Electrical Energy in the EMU

Energy is stored in the EMU through capacitance to infinity and to underlying conductors. The quantity of energy in each of these modes depends on the voltages and capacitances as,

$$E_\infty = \frac{1}{2} C_\infty V^2$$

$$E_{\delta\nu} = \frac{1}{2} C_g (\delta V)^2$$

where δV is the voltage difference between the suit surface material and the suit ground. where V is the surface voltage relative to infinity, and C_∞ is the capacitance to infinity. These capacitances can be estimated by approximating the EMU as a conducting spherical ball with radius R and covered with teflon of thickness d. The capacitance to infinity can then be determined by the definition of capacitance,

$$Q = CV$$

and the relationship between charge and potential on a sphere,

$$V = \frac{Q}{4\pi\epsilon_0 R}$$

This gives for the capacitance of a sphere,

$$C_\infty = 4\pi\epsilon_0 R$$

$$= 10^2 pF \ (1 meter object)$$

The capacitance to the underlying conductor (suit ground) C_g is much larger and can be estimated assuming a parallel plate capacitor of area the surface area of the EMU. The capacitance of a parallel plate capicator is,

$$C_g = k\epsilon_0 \frac{A}{d}$$

where k is the dielectric constant which we will call 1 for these estimates, A is the surface area, and d the thickness of the insulating suit material. For a spherical EMU the surface area is $A = 4\pi R^2$ so the capacitance to suit ground is

$$C_g = 4\pi\epsilon_0 \frac{R^2}{d}$$

which for a 1 meter radius EMU with 1 centimeter of insulating material results in

$$C_g = 10^4 pF$$

Hence $C_g = \frac{R}{d} C_\infty = 100 C_\infty$, so for comparable voltages much more energy is stored in the capacitance to suit ground than in the capacitance to infinity.

The MATCHG calculations showed that the dominant material, teflon, would charge to approximately -4000 volts and that the face plate material would charge to -6000 volts, and the suit ground to about -6800 volts. Hence, $V_\infty = -4000v$ and $\delta V = -1000v$. Using these values E_∞ and $E_{\delta V}$ can be estimated as,

$$E_\infty = 1^{-3} Joules$$

$$E_\delta = .1 Joules$$

These calculations are upper bounds on the energy involved in a discharge because they assume all the stored charge is transferred in the discharge. In realistic discharges only a fraction of the charge (depending on the geometry and the type of discharge) contributes to the discharge.

These estimates can be improved using the results of the NASCAP calculation. The NASCAP code computes the capacitance to infinity for a three dimensional object as part of its charging algorithm. For the EMU NASCAP gives the effective radius of $R_{eff} = .608M$ thus $C_\infty = 68pF$, and $E_\infty = .310^{-3} Joules$.

Two other important points should be made at this point. First, grounding the astronaut would increase the arcing hazard by fixing the suit ground at the shuttle ground. This would increase δV by a factor of three and hence the stored energy by ten fold. Secondly, The charging of the suit ground happens on time scale which is much slower than the other charging times because of the relatively small amount of exposed ground conductor. Hence, for early times (as seen in the NASCAP charging history shown section VI) the differential voltage, δV is over twice the steady state value of 800-1000 volts.

References

1) Gussenhoven,M. S., D. A. Hardy, F. Rich, W. J. Burke and H. C. Yeh, "High-Level Spacecraft Charging in the Low Altitude Polar Auroral Environment," AFGL-TR-85-0291, ADA162145.

2) Ashley, J. C., C. J. Tung, V. E. Anderson and T. H. Ritchie, IEEE Transactions on Nuclear Science, *NS-25/6*, p. 1566, 1978.

3) Darlington, E. H. and V. E. Cosslett, "Backscattering of 0.5-10 KeV Electrons from Solid Targets," *J. Phys. D5*, p. 387, 1959.

4) Yang, K., W. L. Gordon, and R. W. Hoffman, "Electron Yields from Spacecraft Materials," presented at the Spacecraft Environment Interactions Technology Workshop, Colorado Springs, October 4-6, 1983.

5) Alonso, E. V., et al., "Z, Dependence of Ion-Induced Electron Emission from Aluminum, *Phys. Rev. 13*, Vol. 22, No. 1, p. 80, July 1980.